SAND2015-4587C

DOUBLE PLANAR WIRE ARRAYS FROM MID-ATOMIC-NUMBER WIRES AS EFFICIENT RADIATORS AT ENHANCED CURRENT ON ZEBRA

A.S. Safronova, V. L. Kantsyrev, I.K. Shrestha, M.E. Weller, V. V. Shlyaptseva, A. Stafford, M. Lorance
University of Nevada, Reno, NV 89557, USA

C.A. Coverdale, B. Jones, K.M. Williamson
Sandia National Laboratories, Albuquerque, NM, USA*

C.Deeney
NSTec, Las Vegas, NV 89030, USA

A. S. Chuvatin
Laboratoire de Physique des Plasmas, Ecole Polytechnique, Palaiseau 91128, France

International Workshop on Radiation from High Energy Density Plasmas (RHEDP 2015)
(Harvey's Lake Tahoe, Stateline, NV, June 9-12, 2015)

**Sandia National Laboratories is a multi-program laboratory managed and operated by Sandia Corporation, a wholly owned subsidiary of Lockheed Martin Corporation, for the U. S. Department of Energy's National Security Administration under contract DE-AC04-94AL85000*

Sandia National Laboratories

UNR research team (spring 2015)

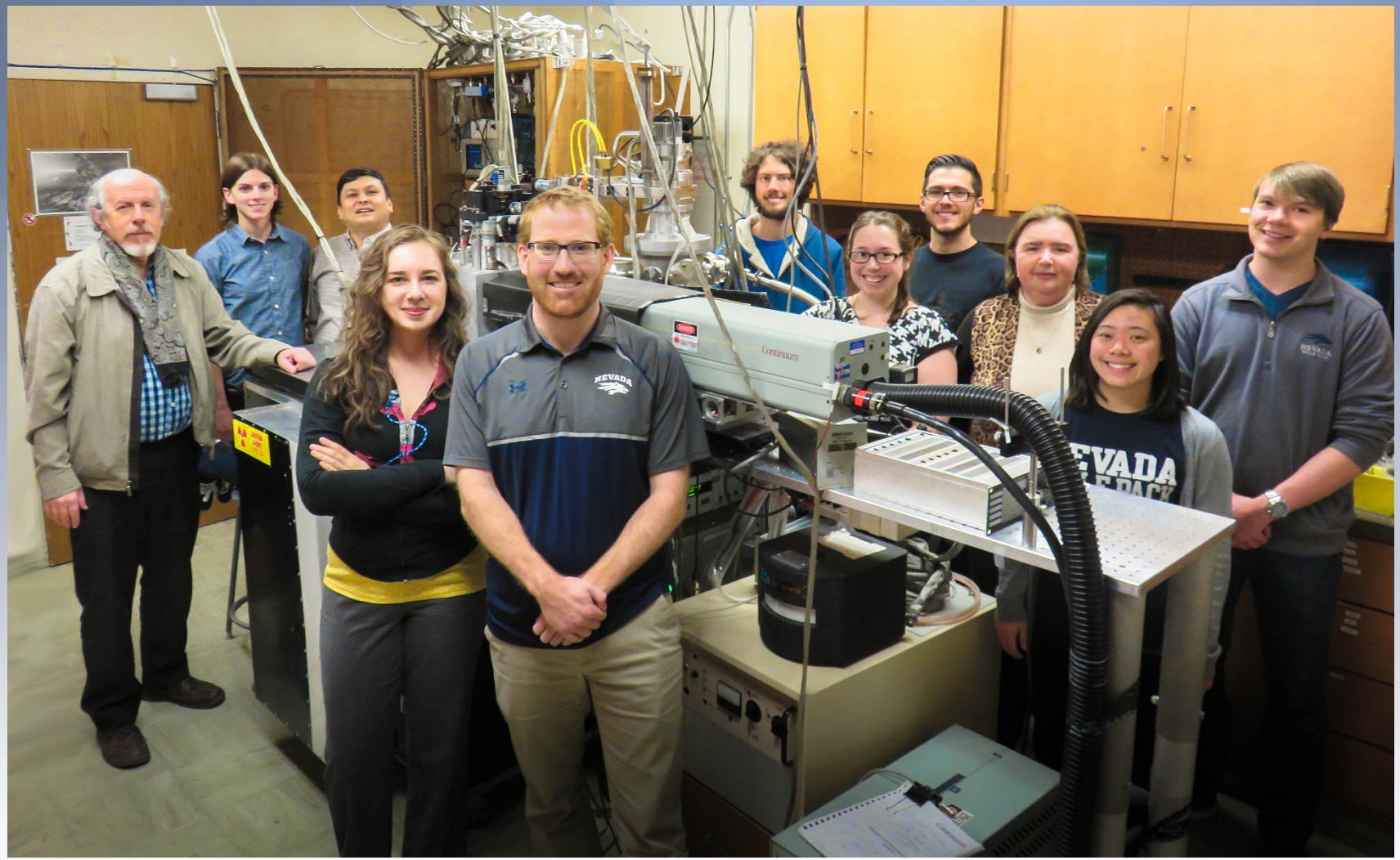

OUTLINE

- Double Planar Wire Arrays (DPWA) at 1 MA current on Zebra
  - a) Brief introduction and motivation
  - b) Implosion dynamics and two types of implosion

- Double Planar Wire Arrays at the enhanced current on Zebra:
  - a) Larger sized DPWAs (Δ=9 mm) with a low aspect ratio (significant foot radiation, no precursor formation in the middle, asymmetry of jets)
  - b) Standard size DPWAs (Δ=6 mm) with a high aspect ratio (formation of precursor in the middle and observation of cold Kα)
  - c) Temporal evolution of K-shell Ni emission. Comparison with Double-Eagle results
  - d) Temporal evolution of L-shell Ni emission. Comparison with Double-Eagle results

Previous Work and Motivation

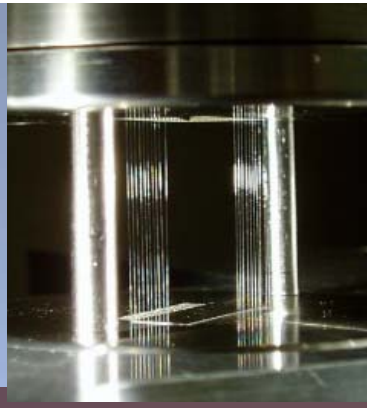

- Double Planar Wire Arrays (DPWA), which consist of two parallel rows of wires, have demonstrated high radiation efficiency (up to 30 kJ), compact size (1.5-3 mm), and pulse shaping capabilities in experiments at 1 MA Zebra[1].

- DPWAs are also very suitable for the new compact multi-source hohlraum concept[2-3].

- It was shown that their implosion dynamics strongly depends on the critical load parameter, the aspect ratio (width to inter-planar gap Δ)[4].

[1] V.L. Kantsyrev *et al*, Phys. Plasmas 15, 030704 (2008)
[2] B. Jones *et al*, Phys. Rev. Let. 104, 125001 (2010)
[3] V.L. Kantsyrev *et al*, Phys. Rev. E, 063101 (2014), also at this workshop
[4] K.M. Williamson *et al*, Phys. Plasmas 17, 112705 (2010)

Diagnostics setup on Zebra

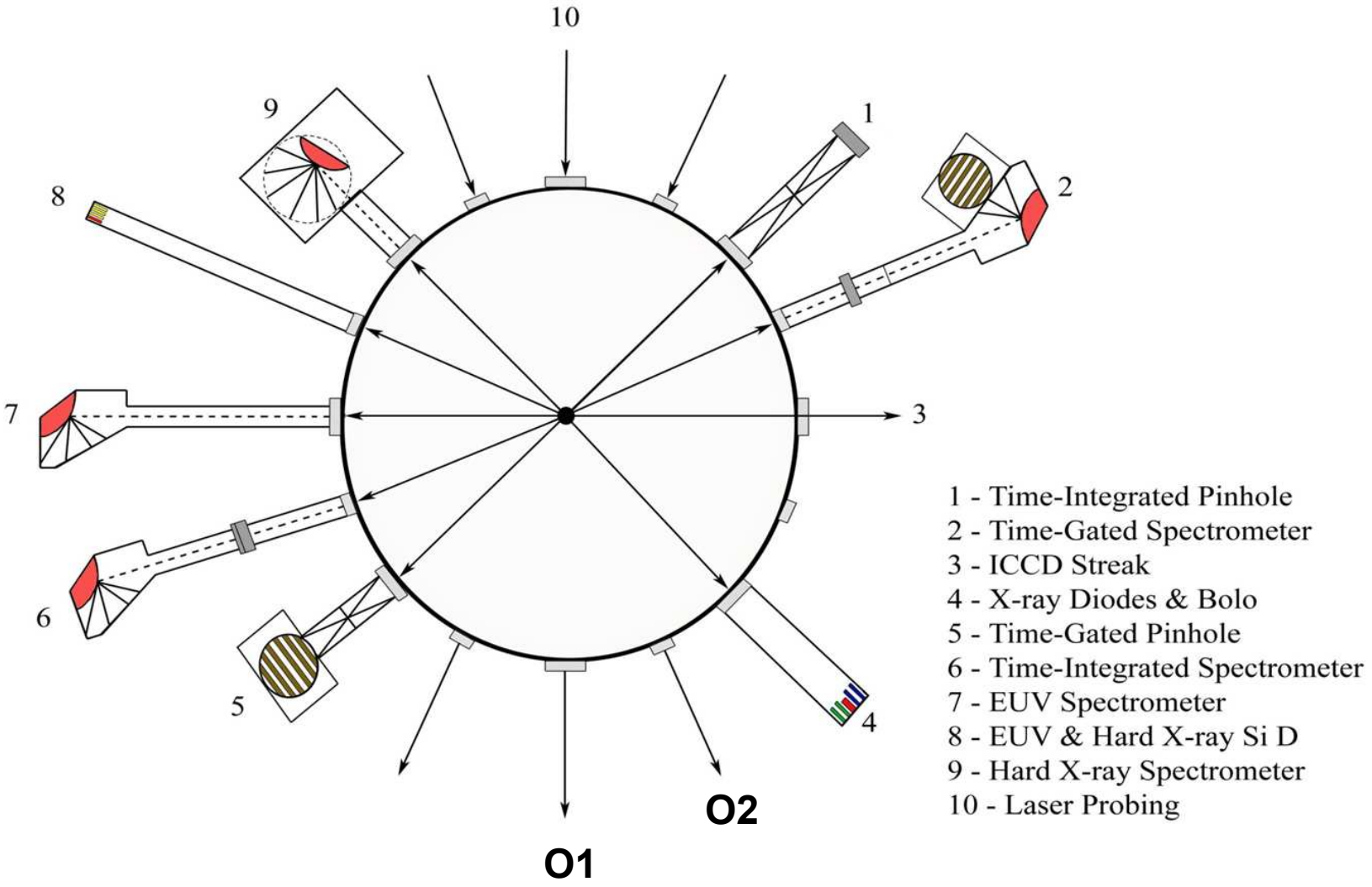

Double Planar Wire Arrays at 1 MA current on Zebra

Alumel DPWA at 1 MA current (shot 1808)

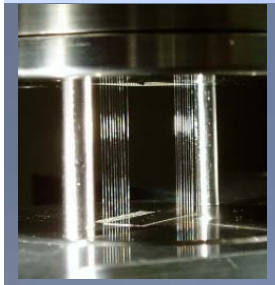

Alumel:
95% Ni,
2% Al,
2% Si

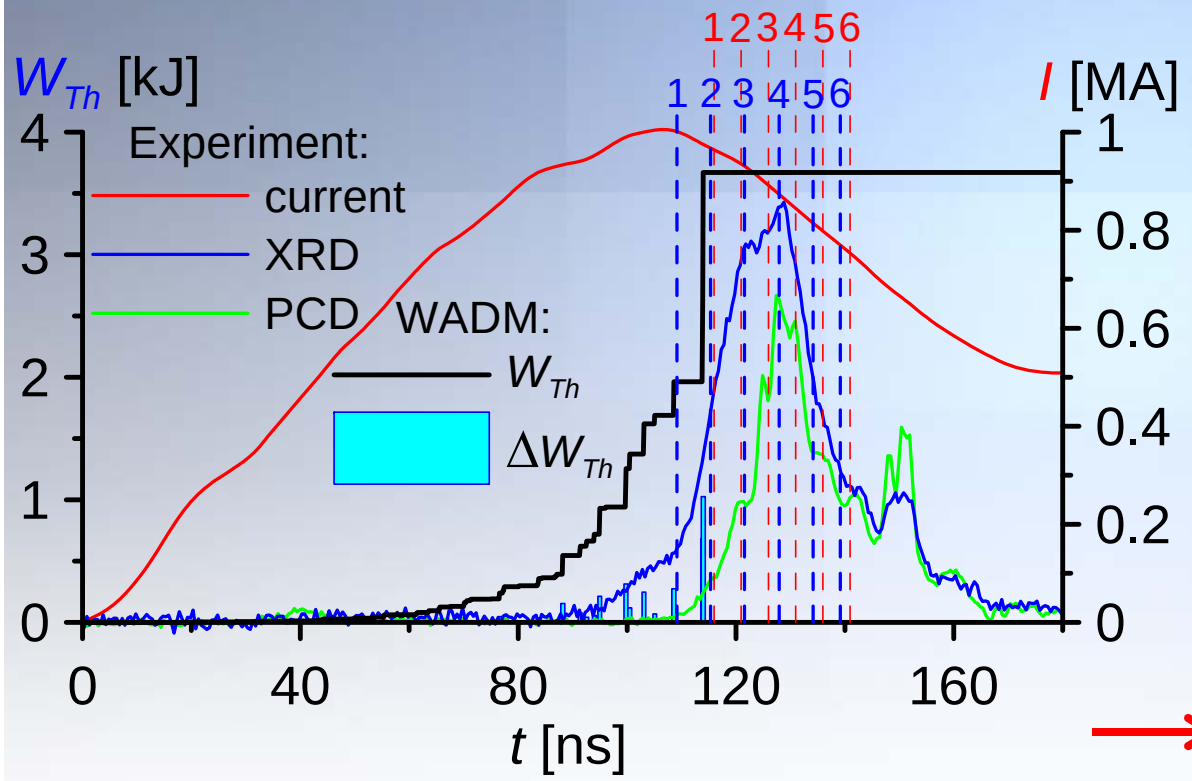

Time-gated pinhole images

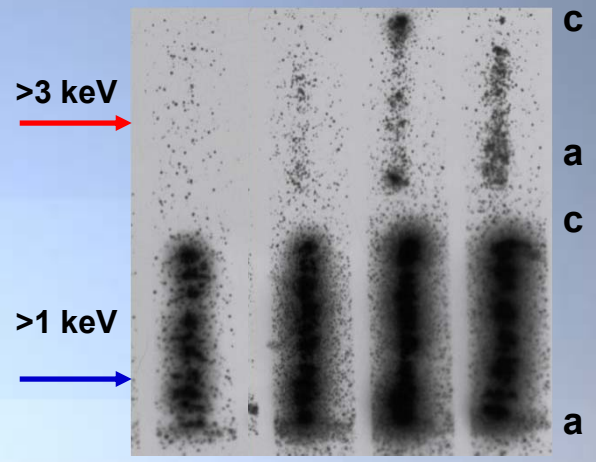

Time-gated K-shell spectra

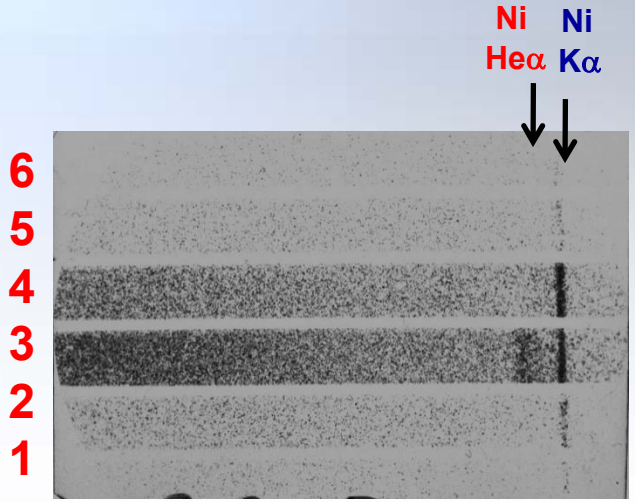

[5]A.S. Safronova et al, IFSA 2009, J. Phys. CS 244, 032031 (2010)

WADM[6] modeling of shot 1808

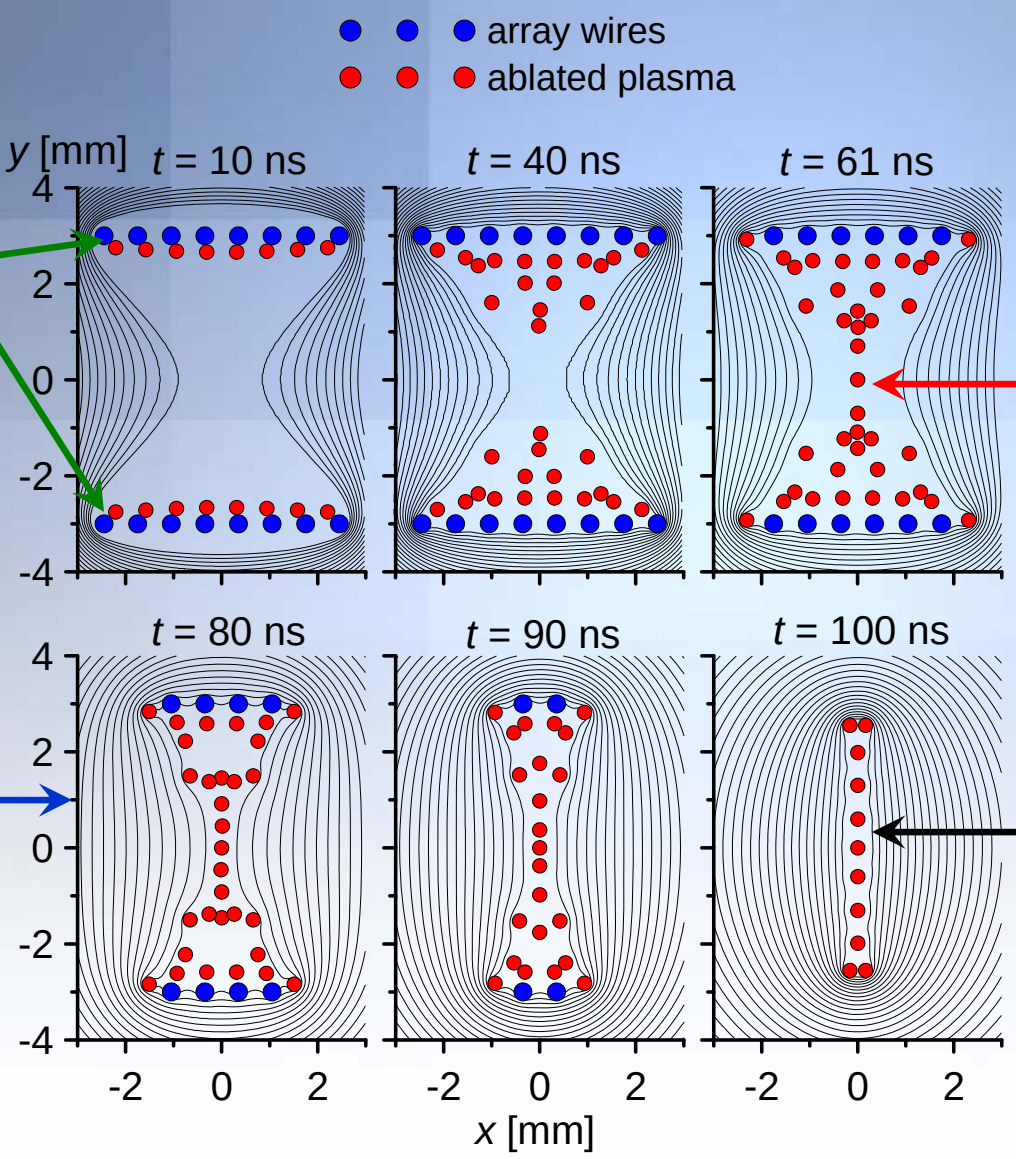

ablation starts

first plasma arrives to the precursor region

ablation cascades toward innermost wires

implosion is almost complete (- 13 ns)

[6]A.A. Esaulov *et al*, HEDP 5, 166 (2009)

Implosion trajectories (shot 1808)

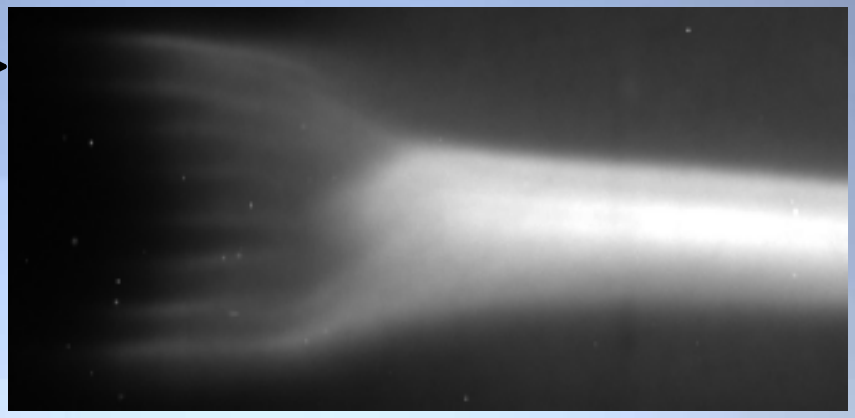

Ablation dynamics at 70 ns

WADM[6] simulation data

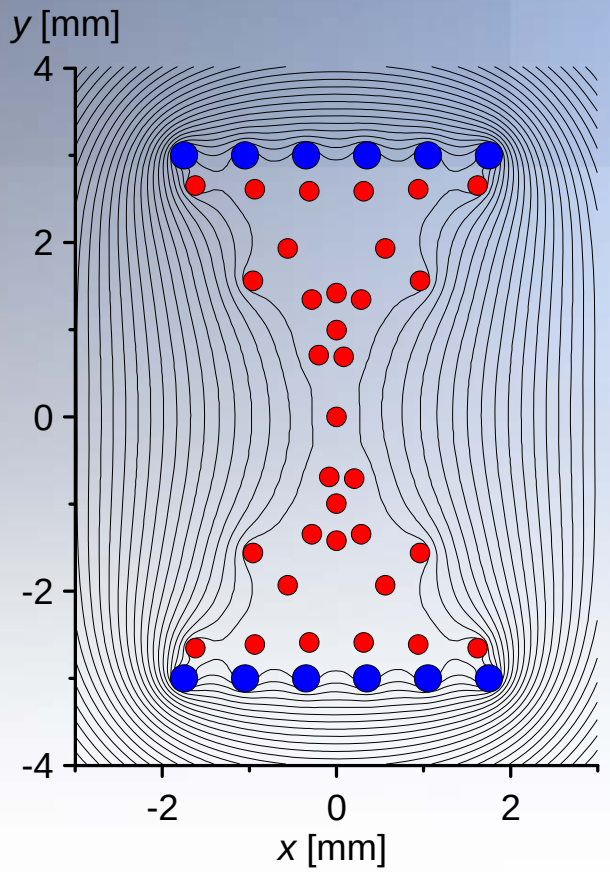

2D (*x*,*y*) density reconstruction

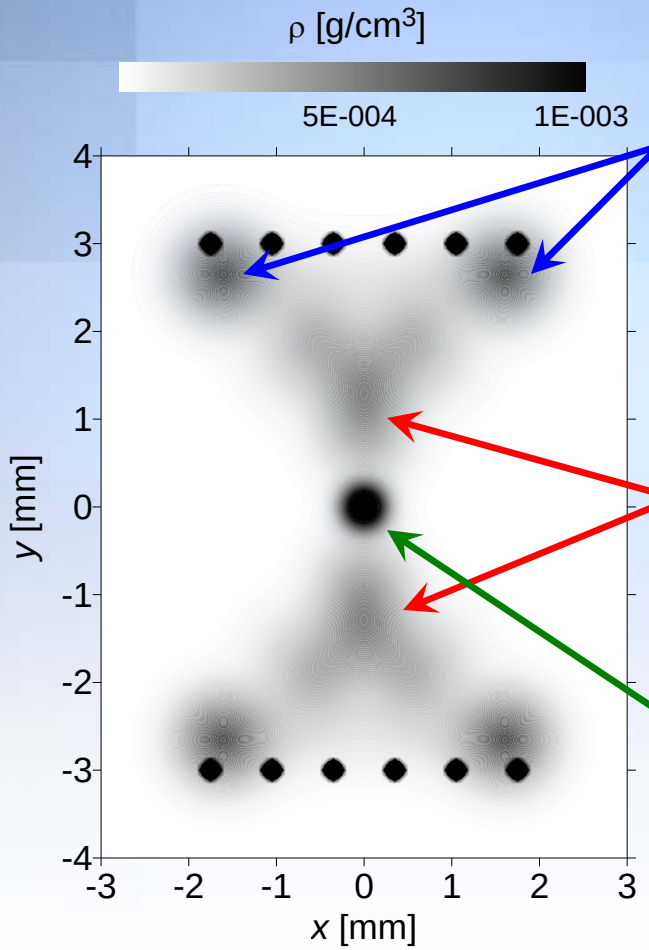

major ablated mass is coming from the outermost wires

global magnetic field cumulates jets creating "*density islands*" apart from the main precursor

precursor is formed by two colliding jets (very different from cylindrical geometry)

[6]A.A. Esaulov *et al*, HEDP 5, 166 (2009)

Comparison with shadowgraphy (shot 1808)

WADM: density integrated along x-axis

t = 70 ns

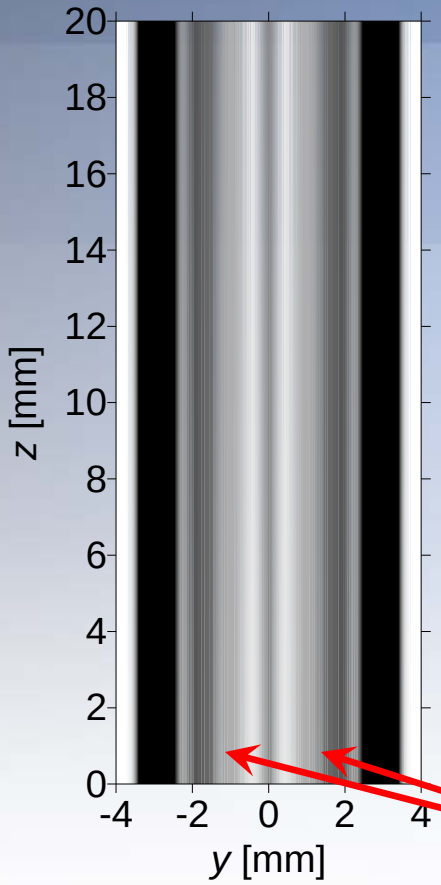

Laser shadowgraphy images

t = 65 ns

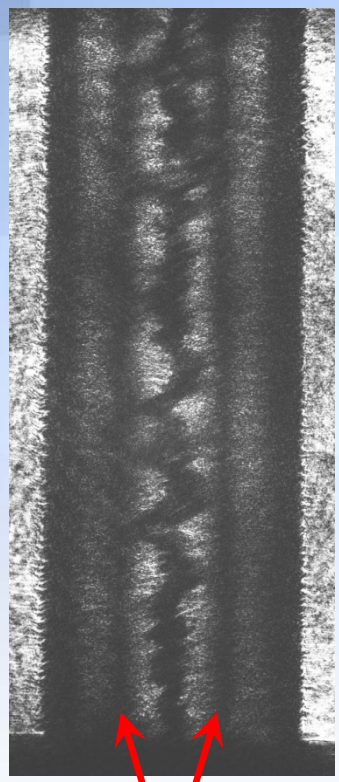

t = 72 ns

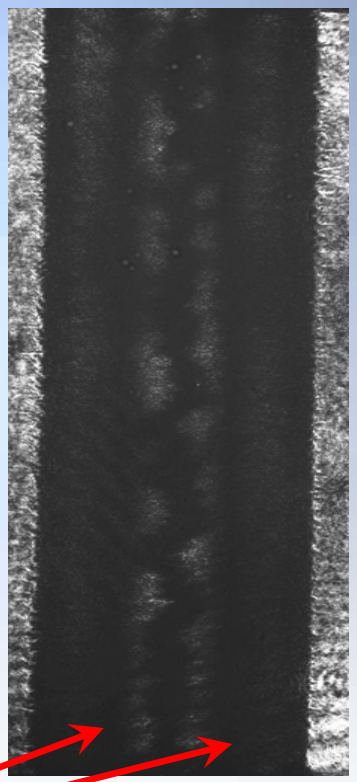

"density islands"

Two different regimes of implosion dynamics in DPWA Z-pinches at 1 MA current[4]

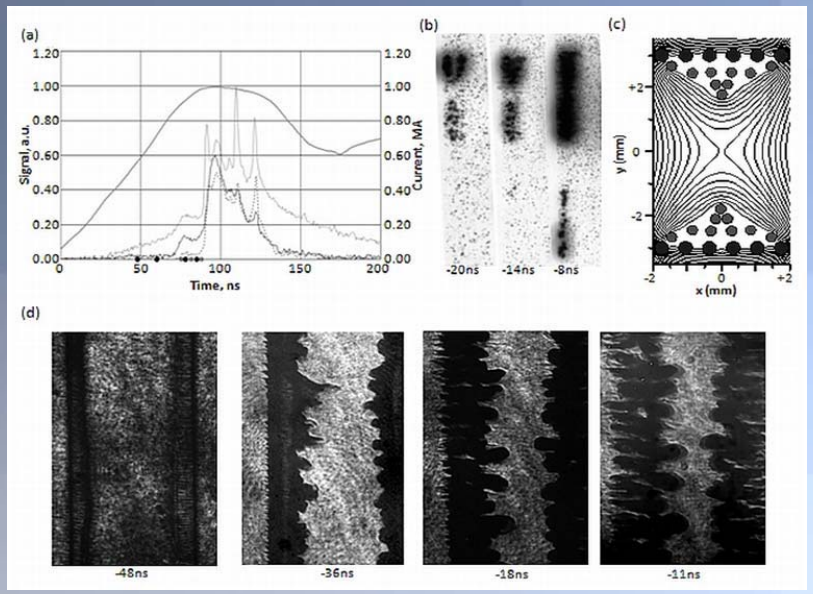

Figure 6 [4]. Shot 1965 DPWA Al (5056): Δ = 6 mm, M = 81 μg/cm, and ϕ = 0.58. Timings are relative to peak XRD power. (a) Experimental signals for shot 1965: current (thick gray), EUV (thin gray), XRD (solid black), and PCD (dotted black) with timing marks for time-gated pinhole (gray squares) and shadowgraphy diagnostics (black circles). (b) Time-gated pinhole images filtered for E > 1000 eV (top) and E > 3000 eV (bottom) with anode on top fielded at 45°. (c) End-on WADM simulation of shot 1965. Dark circles represent the stationary wire cores, the light gray circles represent the streaming coronal plasma, and the lines represent the magnetic field topography. (d) Plane-parallel shadowgraphy with anode on top.

❑ Low aspect ratio loads allow for strong global magnetic field penetration that magnetically confines the ablated plasma from each plane off-axis until few ns before to peak output. The secondary precursors produced significant foot pulse emission.

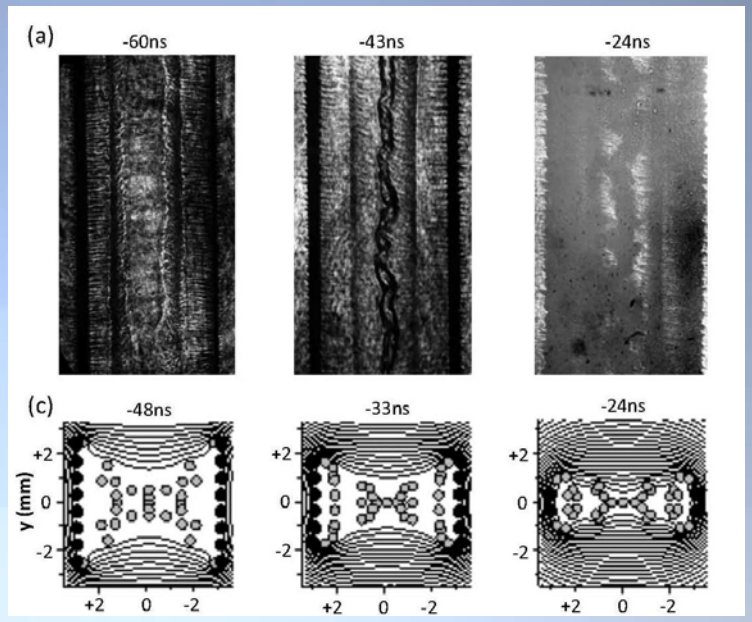

Figure 9 [4]. DPWA Al 5056: Δ =6 mm, M=66 g/cm, and ϕ = 1.1. (a) Plane-parallel laser shadowgraphy images with indicated timings. The first, second, and third images were from shots 2164, 1963, and 1964, respectively. (c) Positions of the array wires black symbols and current filaments representing the ablated plasma gray symbols. The global magnetic topography is shown by the contours.

❑ Intermediate aspect ratio loads allow the global magnetic field to penetrate into the interior of the array without disrupting the formation of the axial precursor. The resulting magnetic topography indicates additional coronal plasma acceleration within the array toward two off-axis points of convergence, one for each plane. This process forms off-axis mass accumulations at these convergence locations that appear to be stationary and uniform until the implosion phase begins.

[4]K. M. Williamson *et al*, Phys. Plasmas 17, 112705 (2010)

Double Planar Wire Arrays at enhanced current on Zebra

Implosion dynamics for larger sized DPWAs (Δ=9 mm) at the enhanced current on Zebra

DPWAs Alumel/Alumel (3104 & 3106)

Shot N	Number of wires	Mass (μg/cm)	t_{impl} (ns)	Bolo (kJ)	Current (MA)	Load details
3104	8x8	115	99	20.41 20.7 20.94	1.54	Alumel (8x10.16μm) 9 mm Alumel (8x10.16μm)
3106	8x8	115	99	20.48 19.8 17.45	1.52	

There are definitely some similarities in signal shapes and shadowgraphy images, in particular closer to the peak of radiation

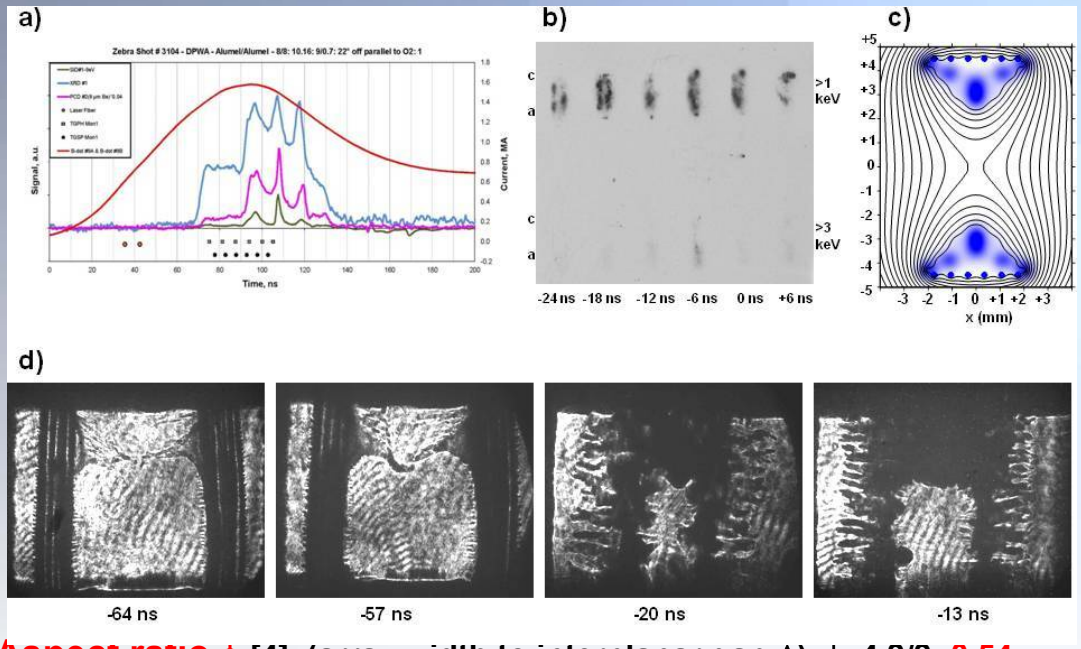

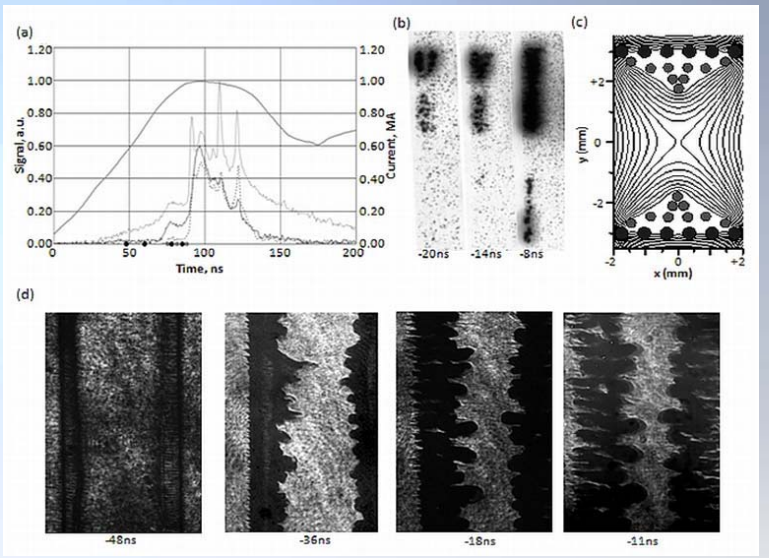

Figure 6 [4]: Shot 1965 DPWA Al (5056): Δ = 6 mm, M = 81 μg/cm, and ϕ = 0.58.

Aspect ratio ϕ [4] (array width to interplanar gap Δ) ϕ=4.9/9=0.54

The low aspect ratio **causes the same effects for larger sized arrays at higher current as at the standard current for arrays with the low aspect ratio ($\phi < 0.7$)[5]:**

- **Such loads allow for strong gmf penetration that magnetically confines the ablated plasma from each plane off-axis for sometime before the peak of XRD**
- **The "so-called" secondary precursor produced significant foot pulse emission**

[4]K. M. Williamson, V.L. Kantsyrev, A.A. Esaulov *et al*, Phys. Plasmas 17, 112705 (2010)

Time-gated imaging and spectroscopy of the larger sized DPWA at the enhanced current on Zebra

DPWA Alumel/Alumel (Δ=9 mm)

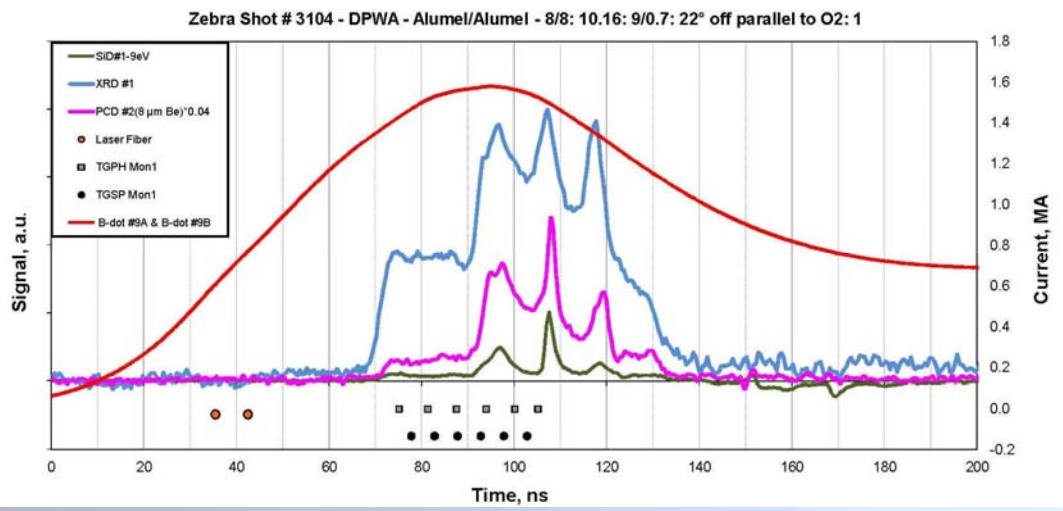

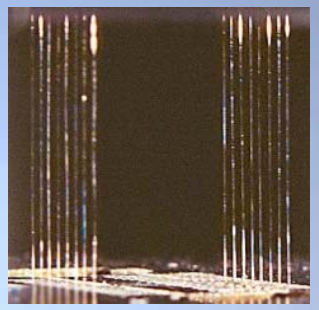

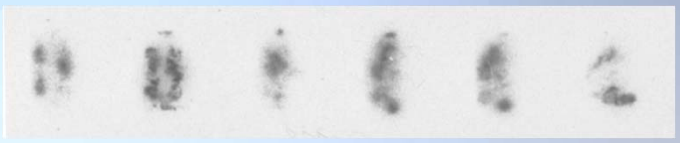

-24 ns -18 ns -12 ns -6 ns 0 ns +6 ns

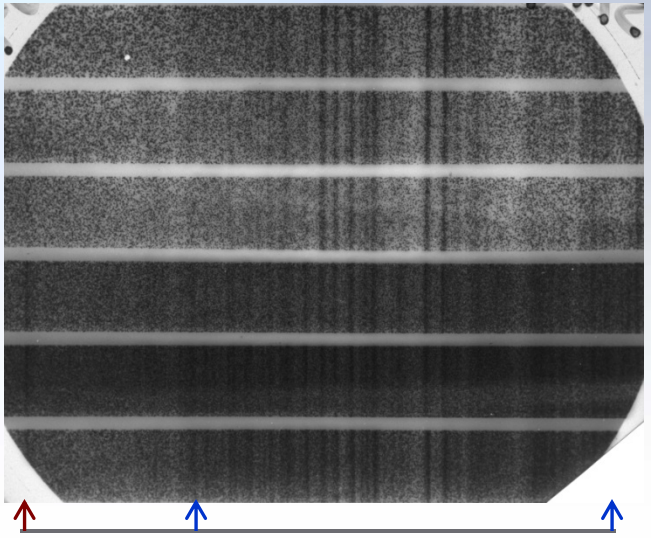

Alumel DPWA (Δ=9 mm):

- ❑ double column are clearly seen 24 and 18 ns before the first x-ray burst in time-gated pinhole images
- ❑very intense time-gated spectra as early as 21 ns before the first x-ray burst

For more about modeling of Alumel PWAs, see

[5]A.S. Safronova *et al*, J. Phys. CP 244, 032031 (2010)
[7]A.S. Safronova *et al*, HEDP 7, 252 (2011)
[8]A.S. Safronova *et al*, IEEE TPS 40, 3347 (2012)

Axial-radiation asymmetry?

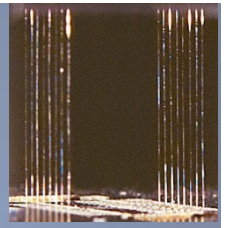

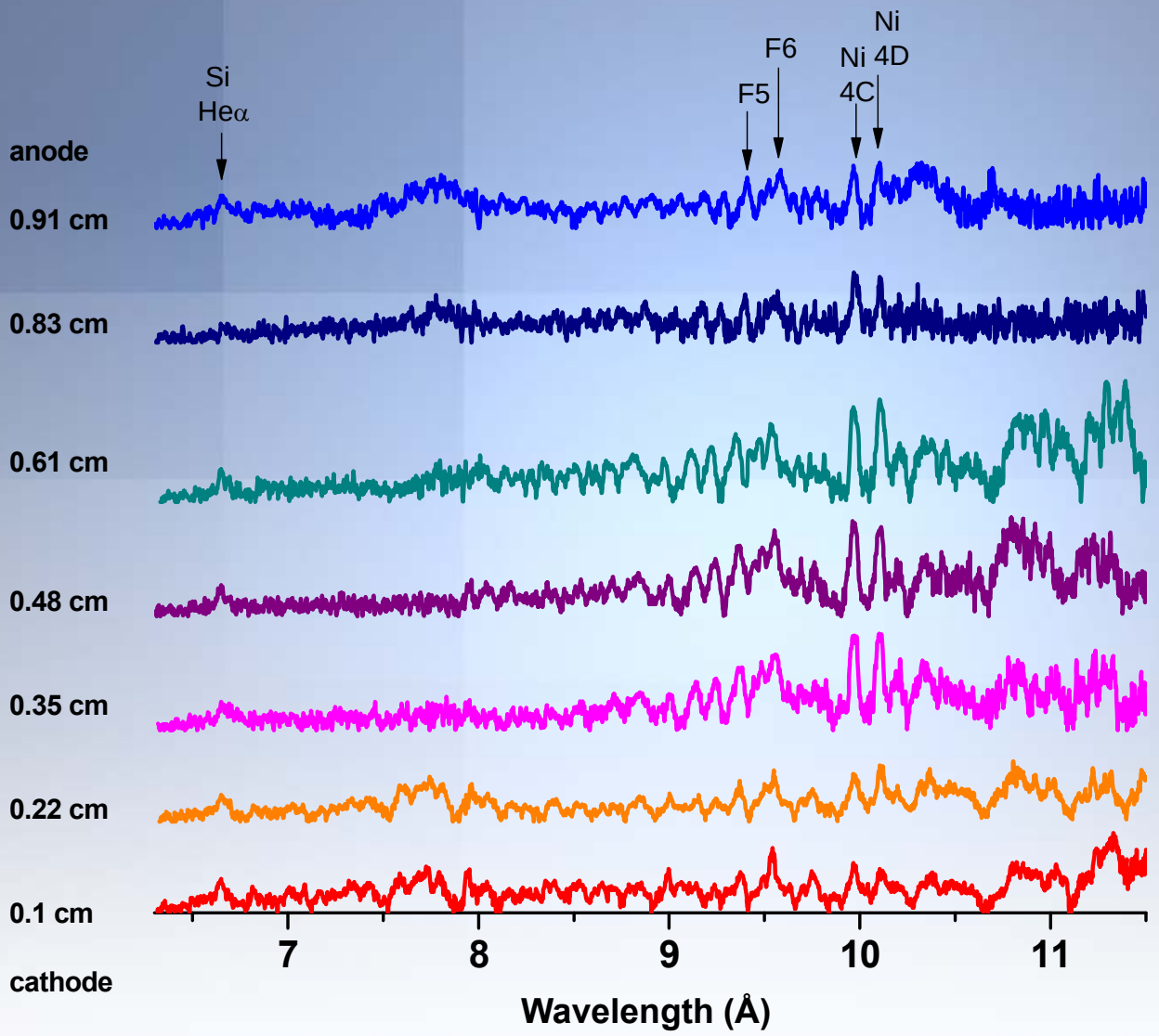

- L-shell Ni spectra are more intense in the middle between the anode and the cathode (Te=360-370 eV) and the weakest near the anode (Te=340 eV)
- More axial asymmetry is observed than for TPWAs. Of the same size.

Implosion characteristics of the standard size DPWAs (Δ=6 mm) at the enhanced current

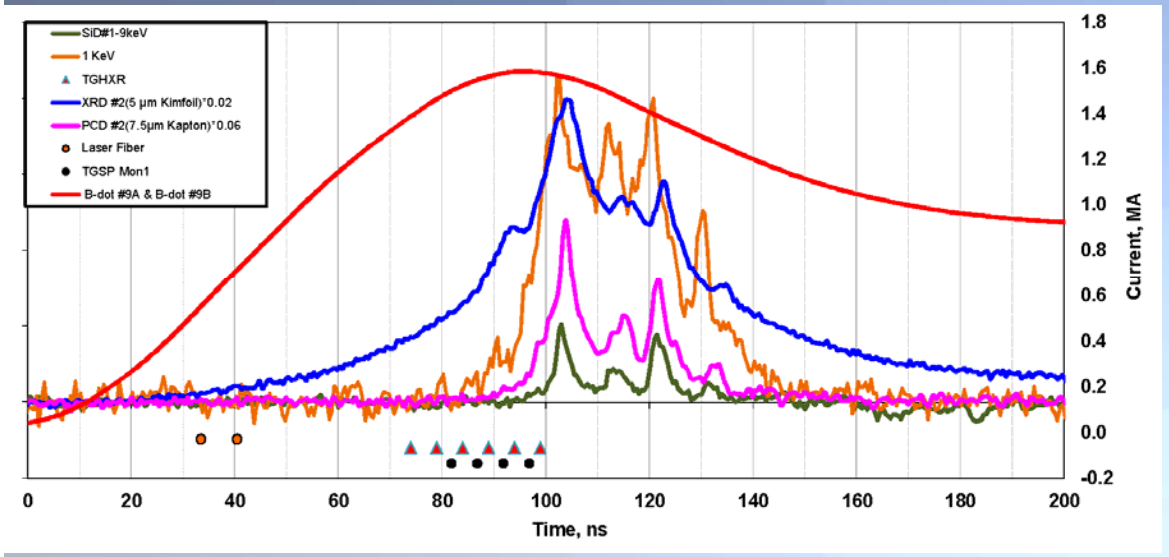

Alumel DPWA (shot 3253)
12x12 (10.7μm), M=192 μg
I=1.58 MA, t_{imp}= 103 ns
early timing for TGSP

Alumel DPWA ((shot 3254)
12x12 (10.16μm), M=173 μg
I=1.62 MA, t_{imp}= 98 ns
later timing for TGSP

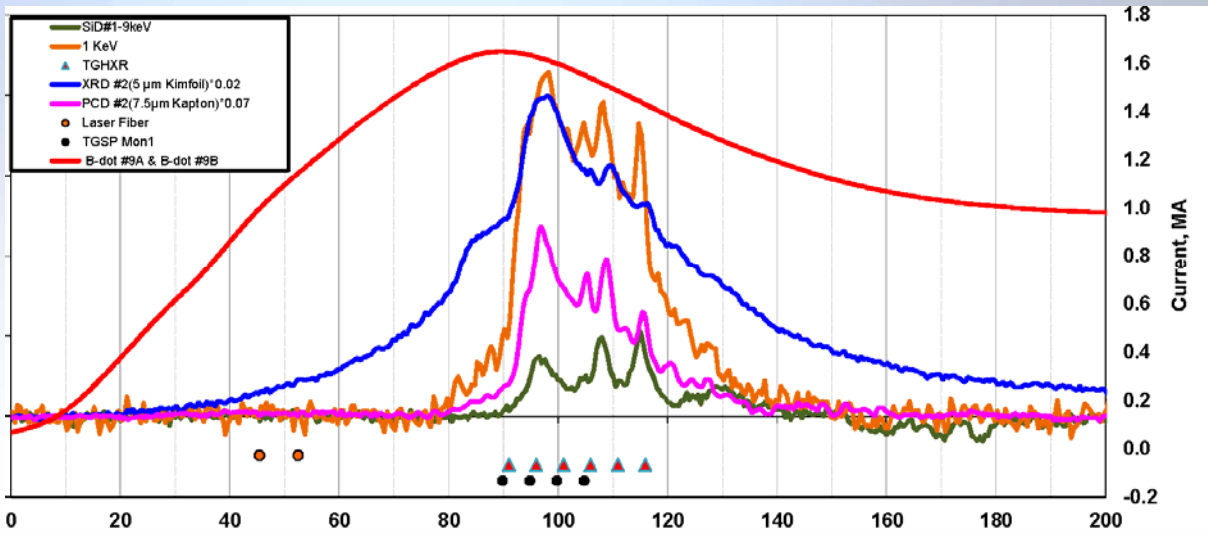

DPWA Alumel/Alumel with different inter-plane gap at enhanced current:

Δ=6 mm and intermediate aspect ratio 1.28: precursor formation in the middle;

Δ=9 mm and low aspect ratio 0.54: asymmetric jets and no precursor formation in the middle

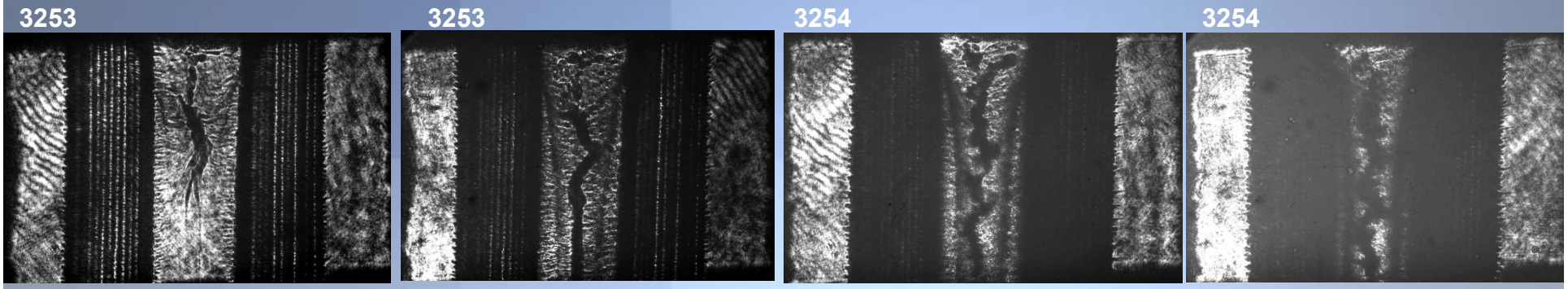

-70 ns -63 ns -53 ns -46 ns

DPWAs Alumel/Alumel (Δ=6 mm)

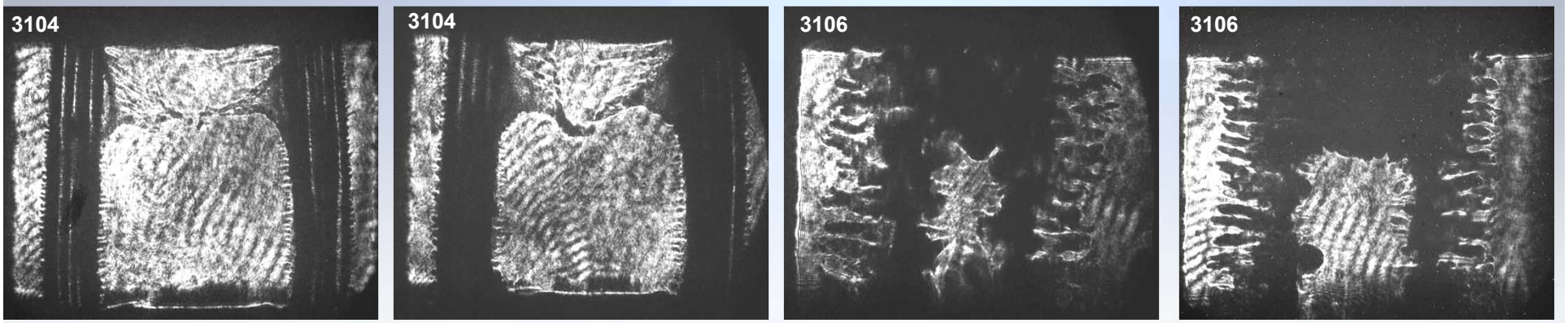

-64 ns -57 ns -20 ns -13 ns

DPWAs Alumel/Alumel (Δ=9 mm)

Anode is at the top. AK gap is 1 cm. Time is from the peak of the XRD signal (X-ray burst).

Time-gated imaging and spectroscopy of standard size DPWAs

Shot 3253: TGSP early in time (both K-shell and L-shell)

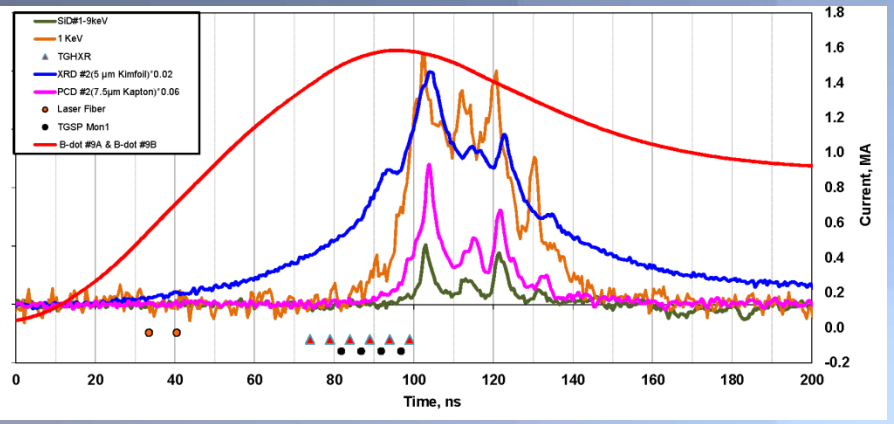

Shot 3254: TGSP later in time (both K-shell and L-shell)

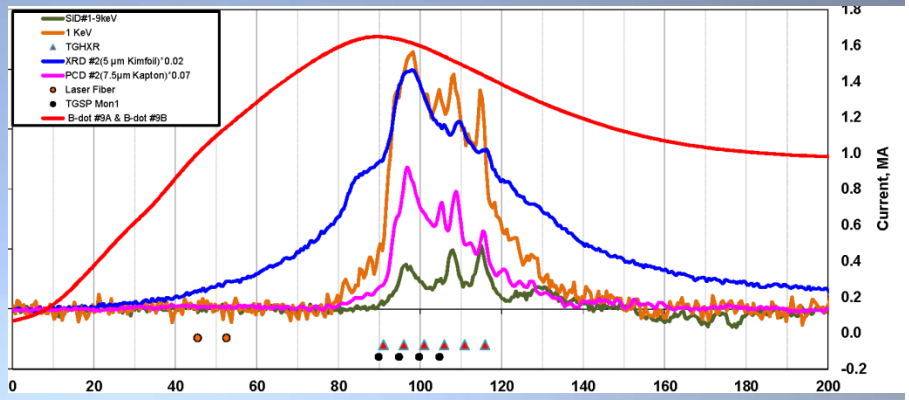

L-shell Ni

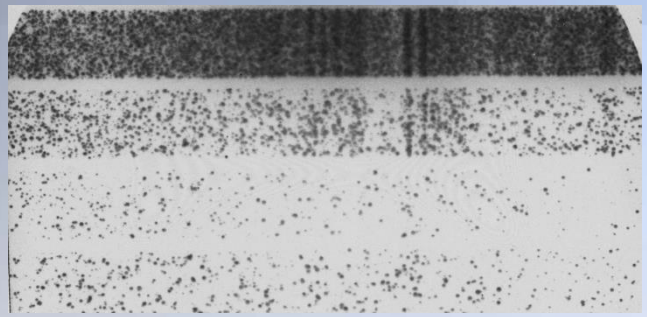

-6 ns

-11ns

L-shell Ni

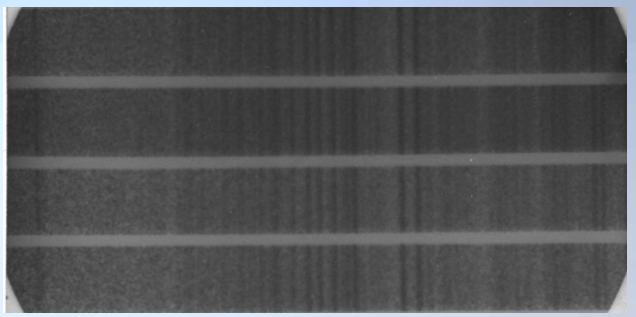

+7 ns

+2 ns

-3 ns

-8 ns

K-shell Ni

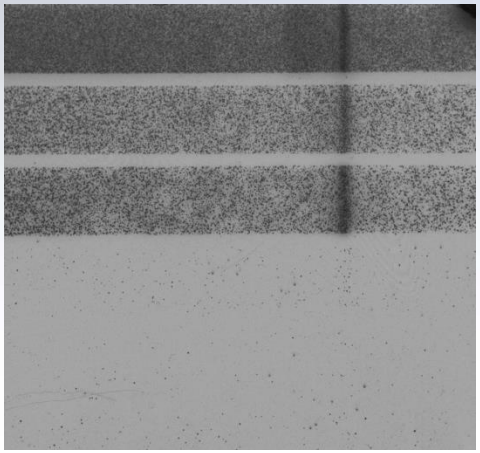

-4 ns

-9 ns

-14 ns

E(Ni Kα)=7478 eV
E(Ni Kβ)=8265 eV

No Heα but cold Kα line and evolution of higher ionization stages

K-shell Ni

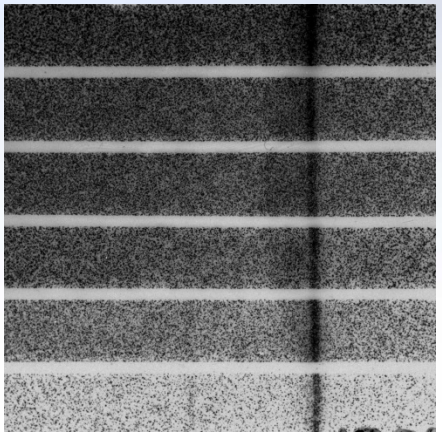

+18 ns

+13 ns

+8 ns

+3 ns

-2 ns

-7 ns

Temporal evolution of K-shell Ni emission

Alumel DPWA at 1 MA current (shot 1808)

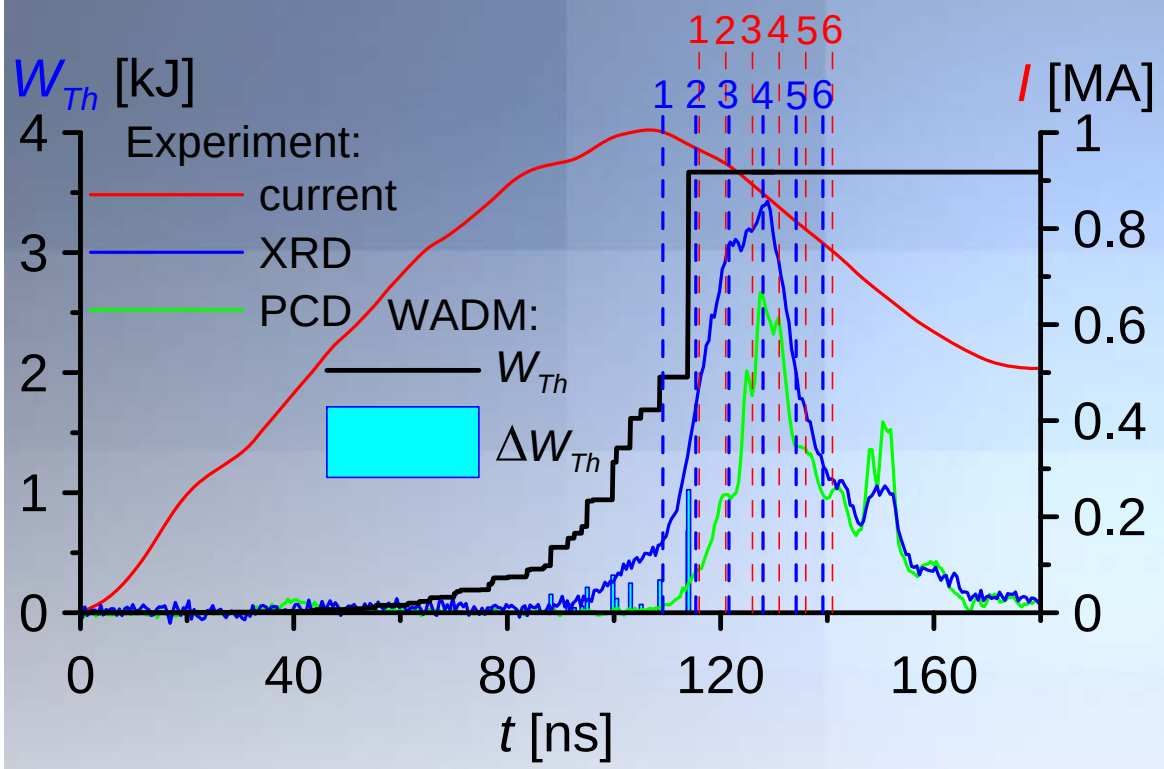

Time-gated pinhole images

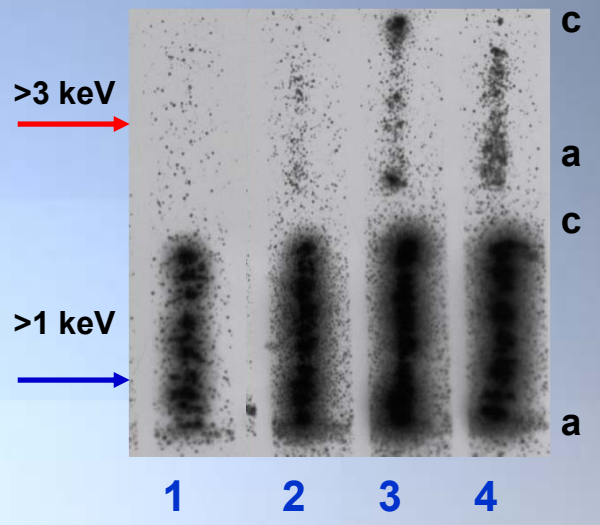

Time-gated K-shell spectra

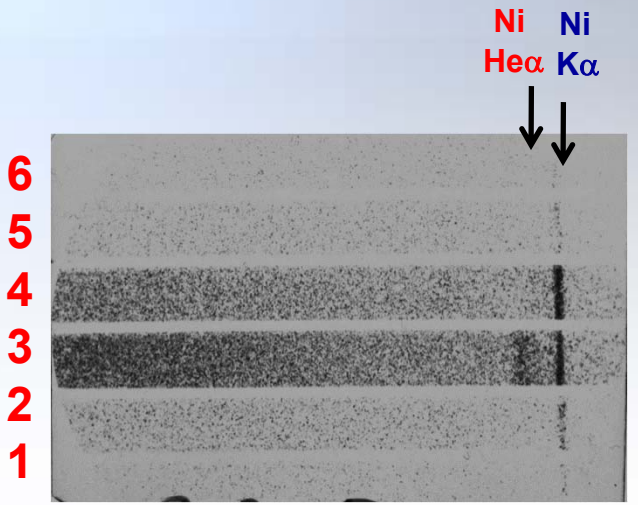

Hot plasma recorded on the frame 3 (at the peak of XRD signal) manifests through the appearance of Ni Heα? line which correlates well with the pinhole image

What ionization stages contribute to K_α at earlier times (before XRD/PCD peak) in experiments at the enhanced current?

Temporal evolution of K-shell Ni emission

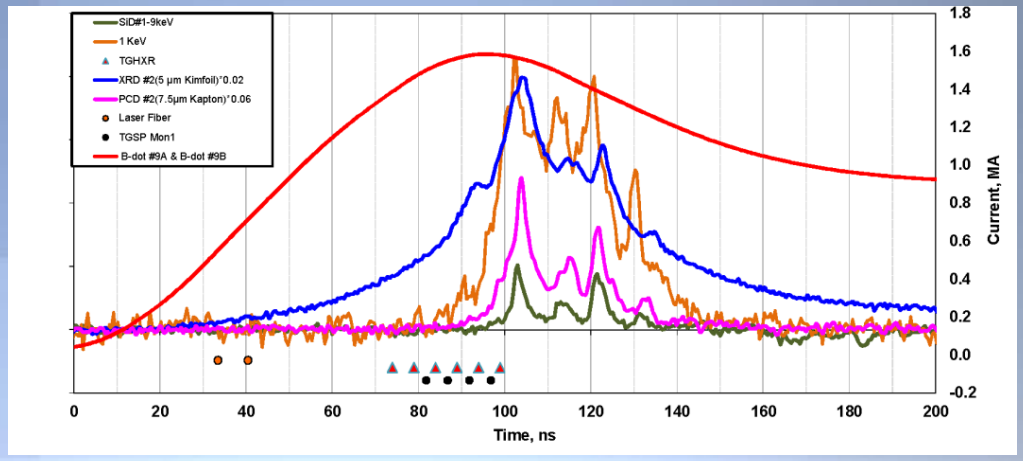

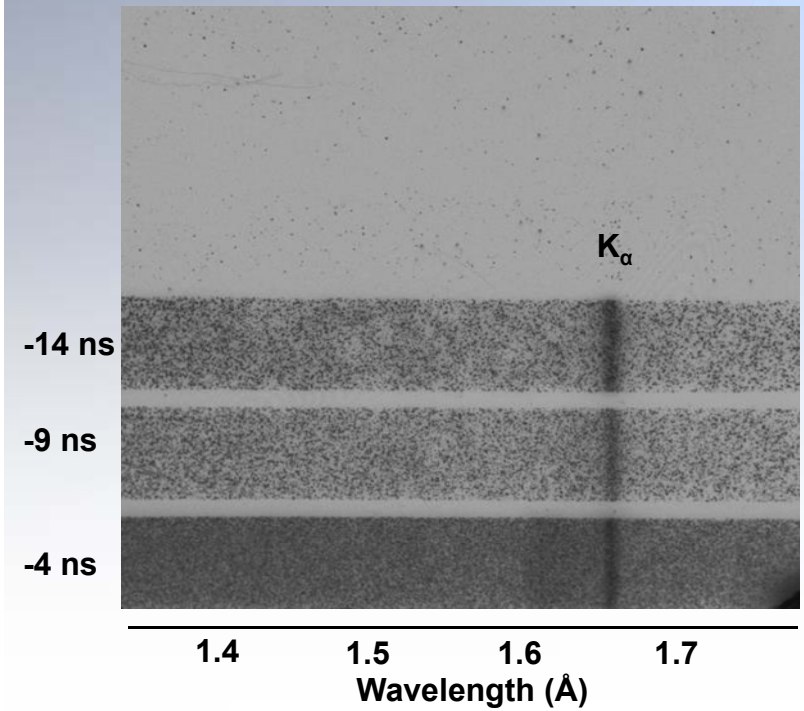

- from – 29 ns to -19 ns: no K_α is observed
- at -14 ns: F-like and less intense O-like ions
- at -9 ns: F- to N-like and less intense C-like ions
- at -4 ns: less intense but all ions from F- to Li-like ions

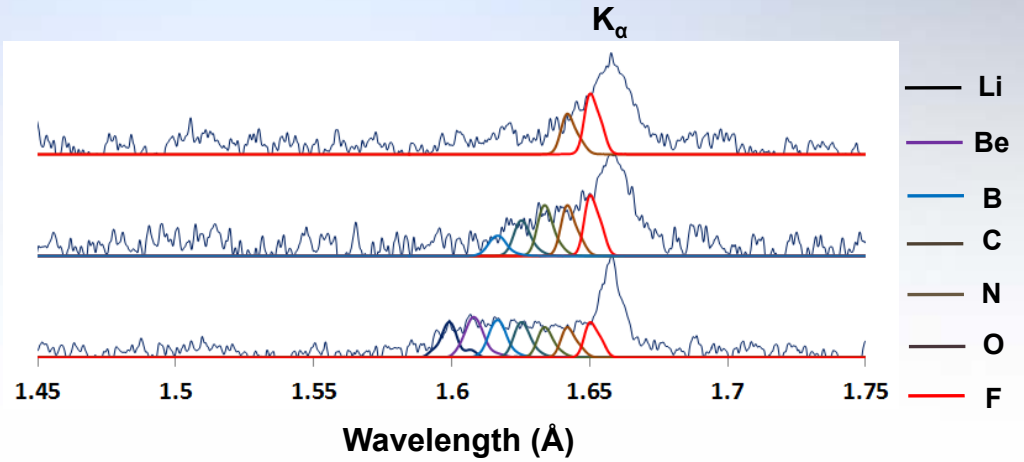

What ionization stages contribute to K_α at later time (before and after XRD/PCD peak) in experiments at the enhanced current?

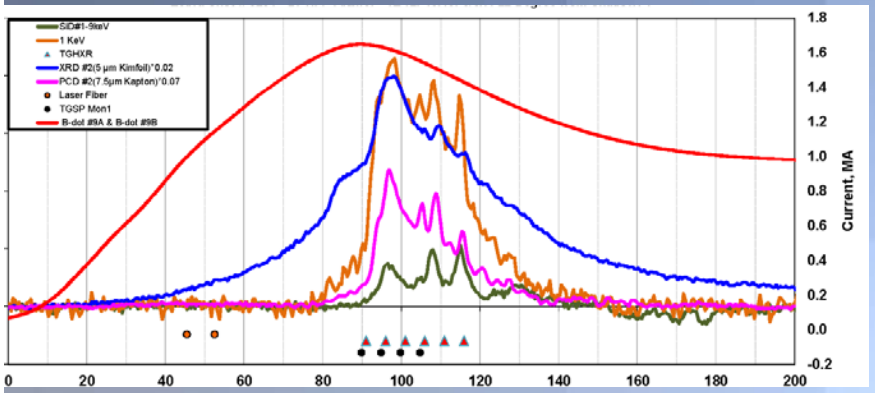

- ❑ at -7 ns: no additional ions are observed
- ❑ at -2 ns: F- and O-like and less intense from N- to B-like ions
- ❑ at +3 ns: F- to Be-like with more intense from N- and C-like ions
- ❑ at +8 ns: all ions from F- to Li-like of the same intensity
- ❑ at +13 ns: all ions from F- to Li-like with less intense from Be- and Li-like ions
- ❑ at +18 ns: non-intense from F- to C-like ions

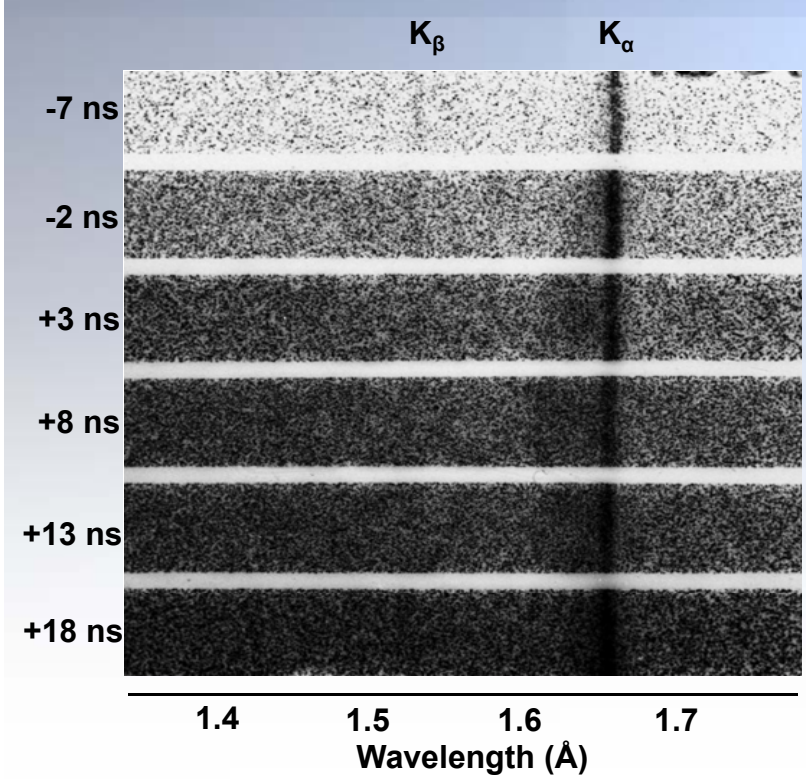

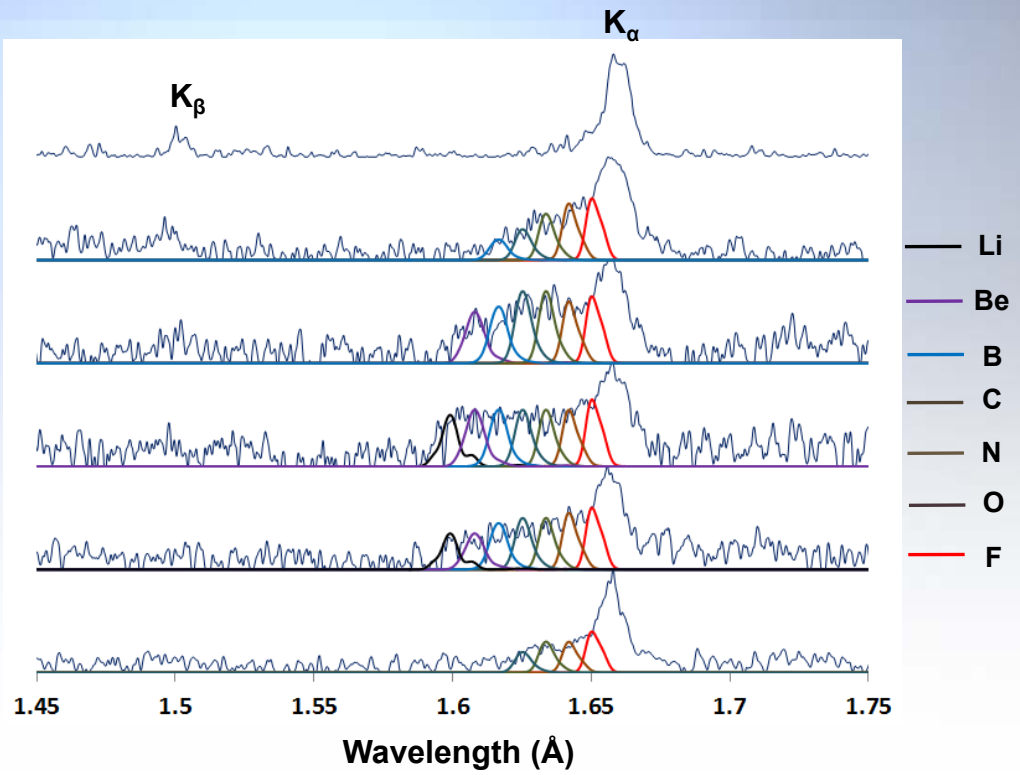

Summarizing: what ionization stages contribute to K_α before and after XRD/PCD peak in experiments at the enhanced current?

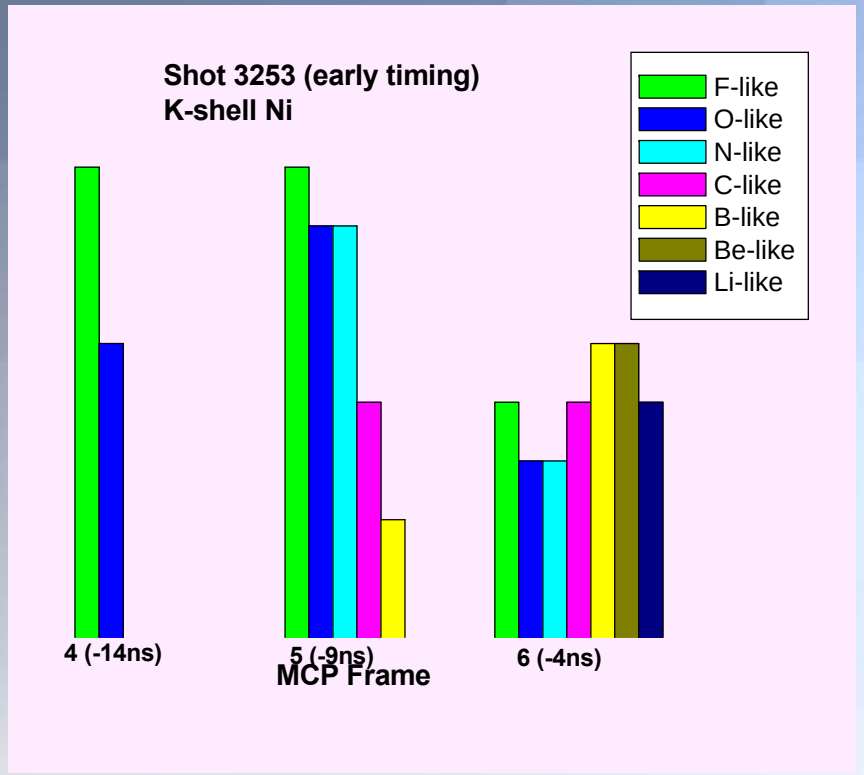

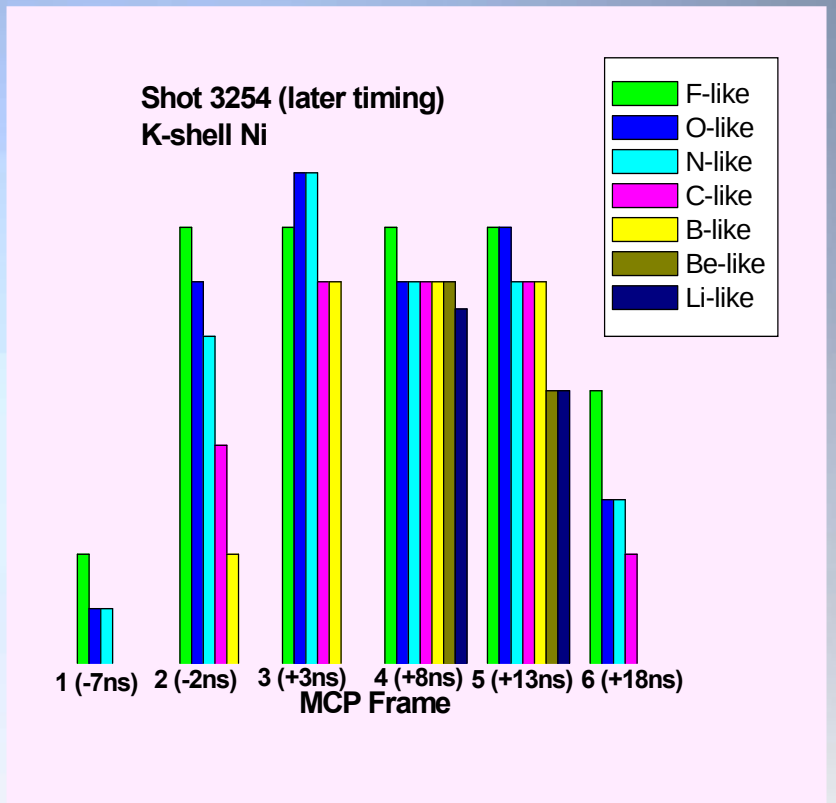

- Only few ionization stages contribute earlier in time (frames 4 and 5 of shot 3253 and frame 1 of shot 3254)
- During the last frame of shot 3253 and from frame 3 up to 5 of shot 3254, the ionization balance is spread out over the large number of ions

Comparison with the results at 4 MA current on Double-EAGLE[9]

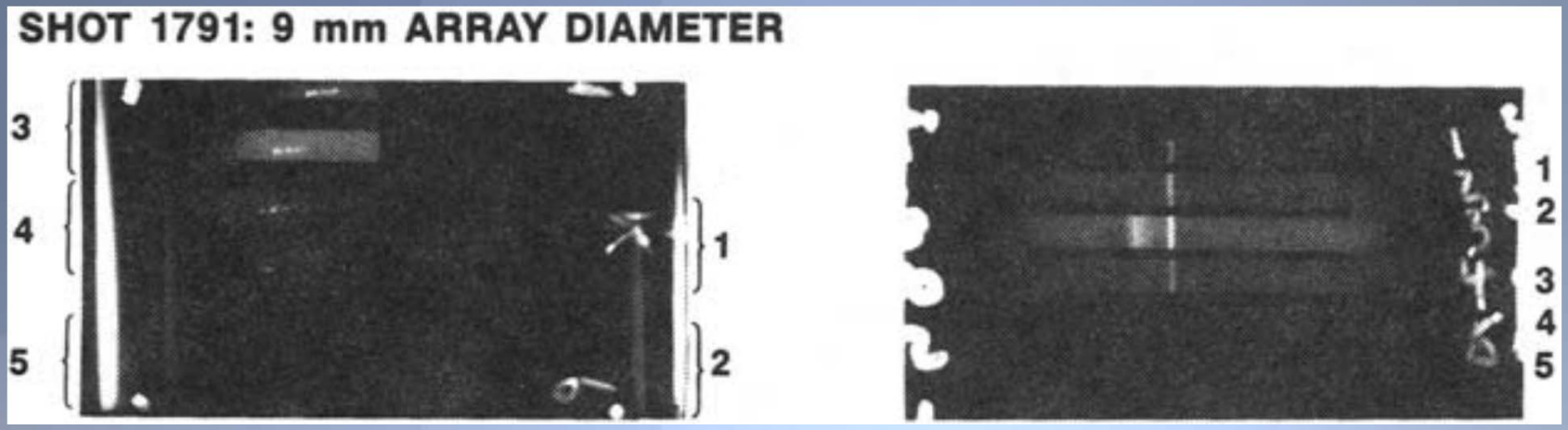

TIME RESOLVED PINHOLE CAMERA (> 7 keV) TIME RESOLVED CRYSTAL SPECTROMETER

Figure 4 [9]. Time-Resolved K-Shell Spectra and Filtered Pinhole Photographs: 9 mm Array.

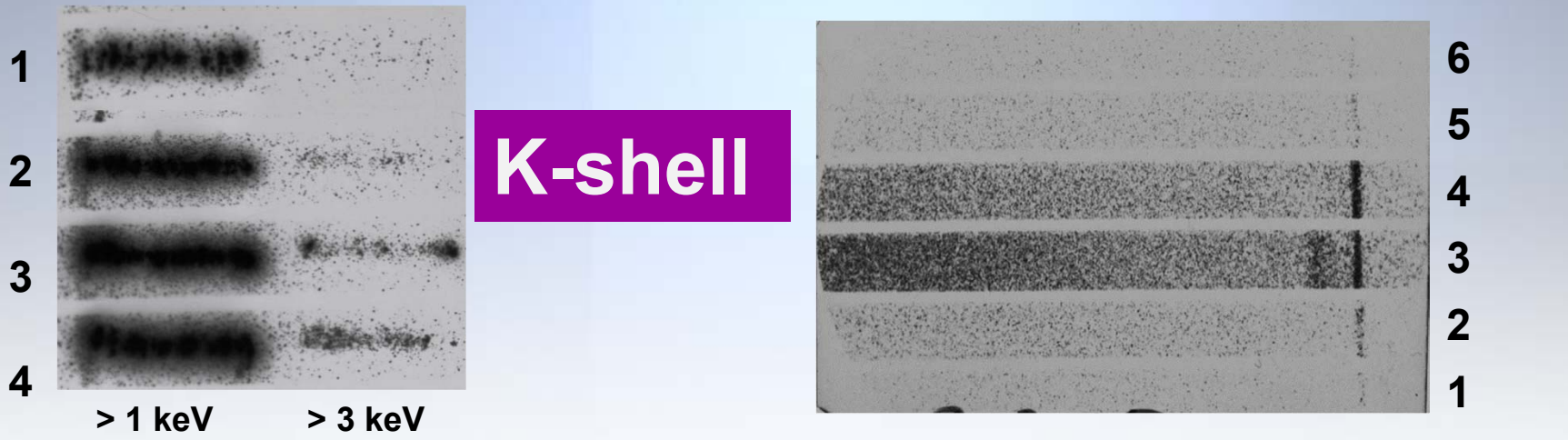

TIME RESOLVED PINHOLE CAMERA TIME RESOLVED CRYSTAL SPECTROMETER

DPWA (Δ=6 mm) experiments at 1 MA current

[9]C. Deeney *et al*, AIP Conference Proceedings 195, 62 (1989)

Temporal evolution of L-shell Ni emission

What ionization stages contribute to L-shell Ni spectra at earlier times (before XRD/PCD peak)?

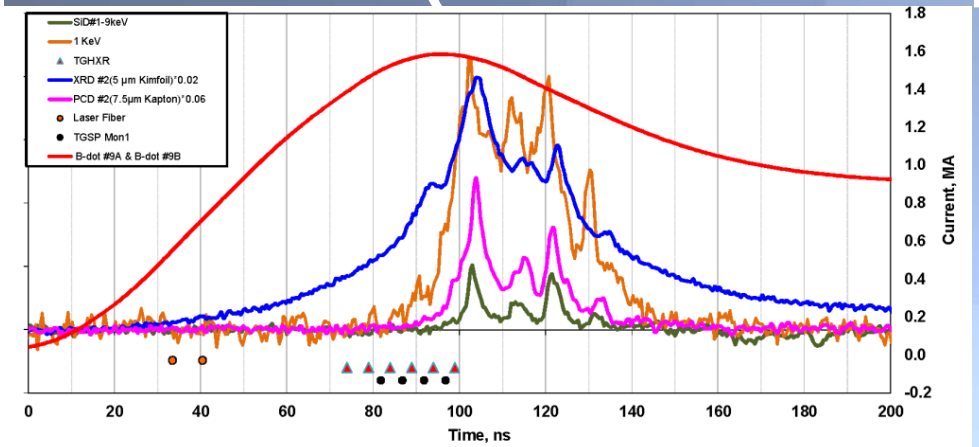

Temporal evolution of L-shell Ni emission

- from – 21 ns to -16 ns: no L-shell spectra
- at -11 ns: intense from Ne-like Na-like ions
- at -6 ns: intense Ne-like and less intense from Na-like and from F- to N-like and even less intense from C-like ions

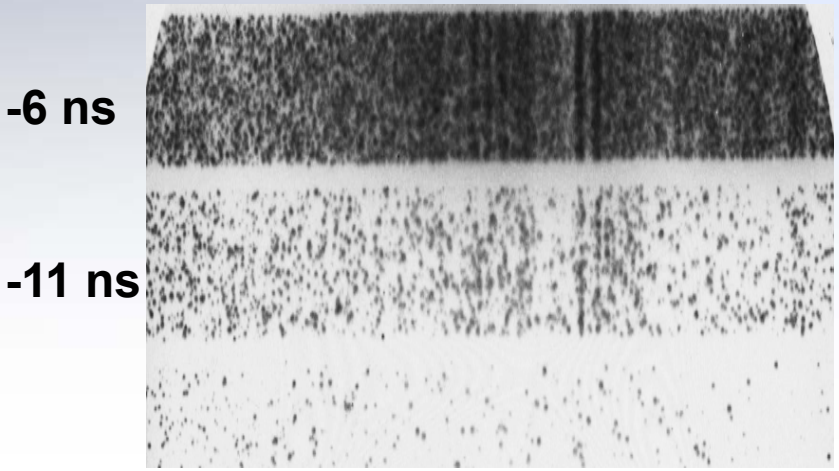

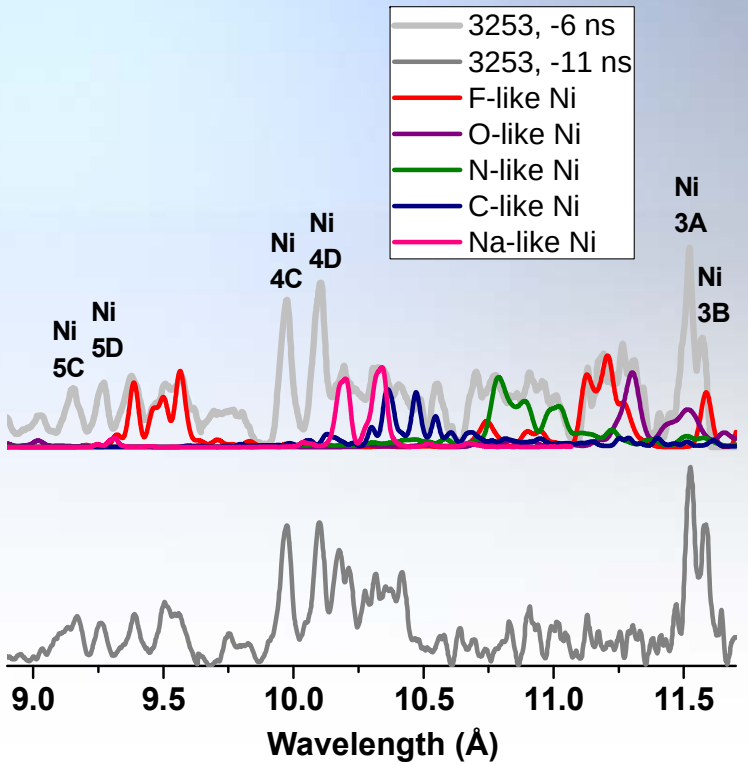

What ionization stages contribute to L-shell Ni spectra at later times (before and after the XRD/PCD peak) in experiments at the enhanced current on Zebra?

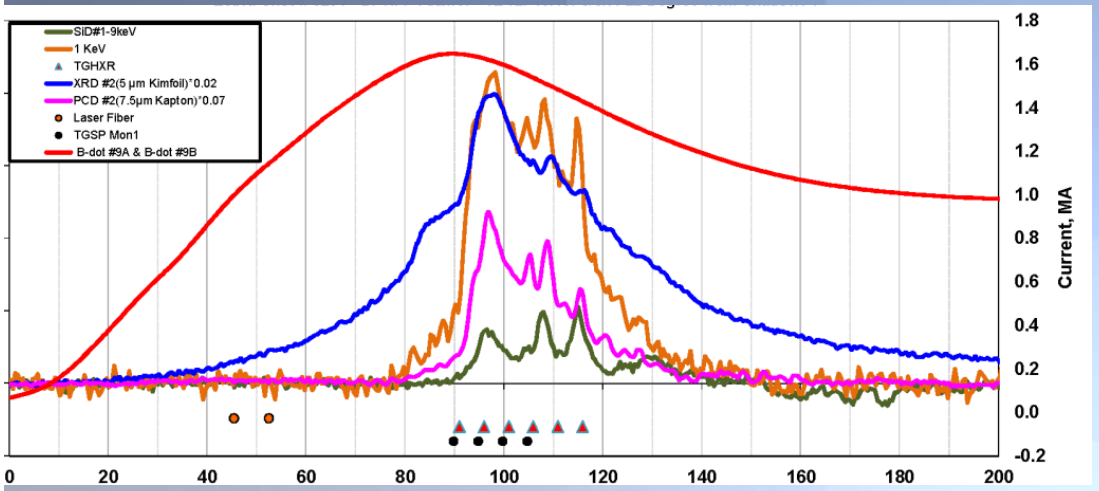

Taking a close look at the contribution from different ions on the next slide

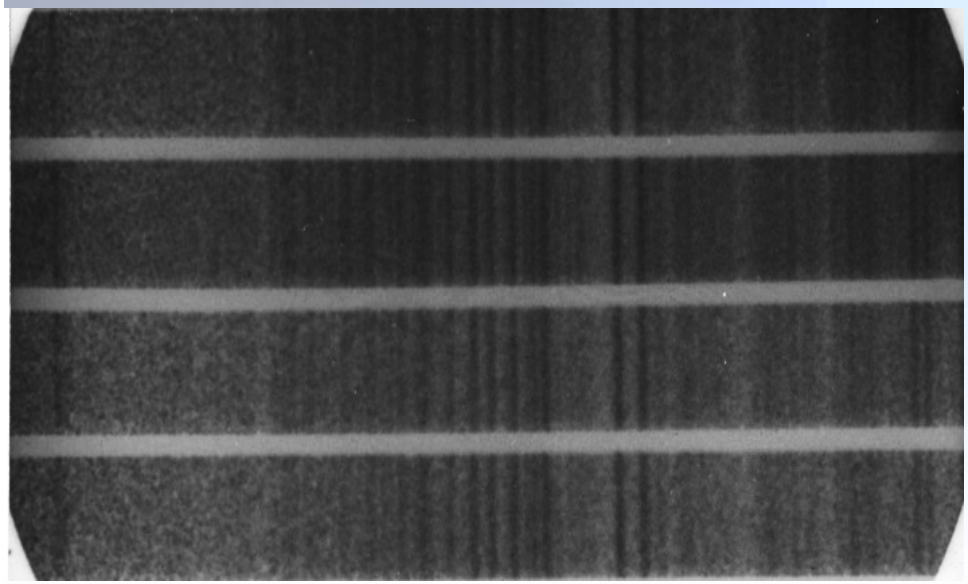

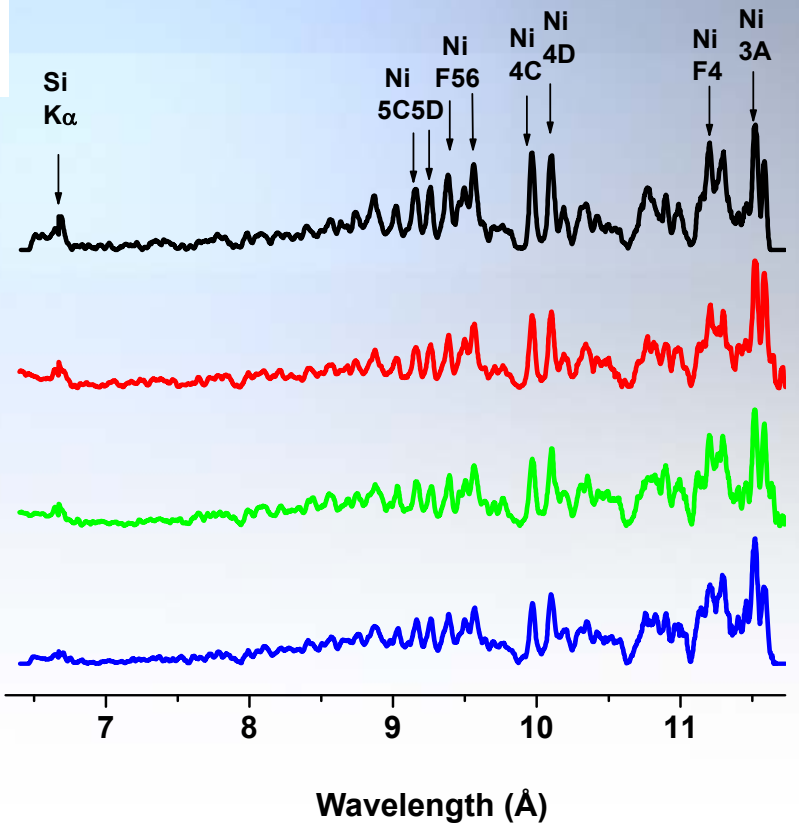

What ionization stages contribute to L-shell Ni spectra at later times (before and after the XRD/PCD peak) in experiments at the enhanced current on Zebra?

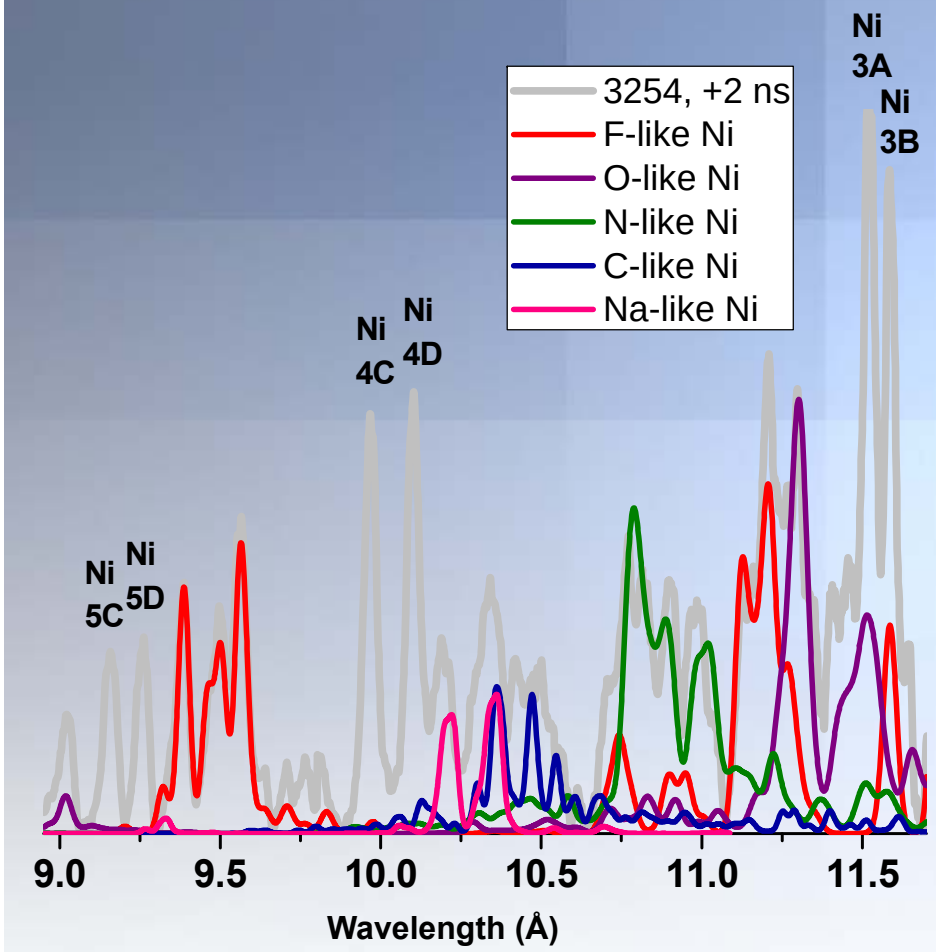

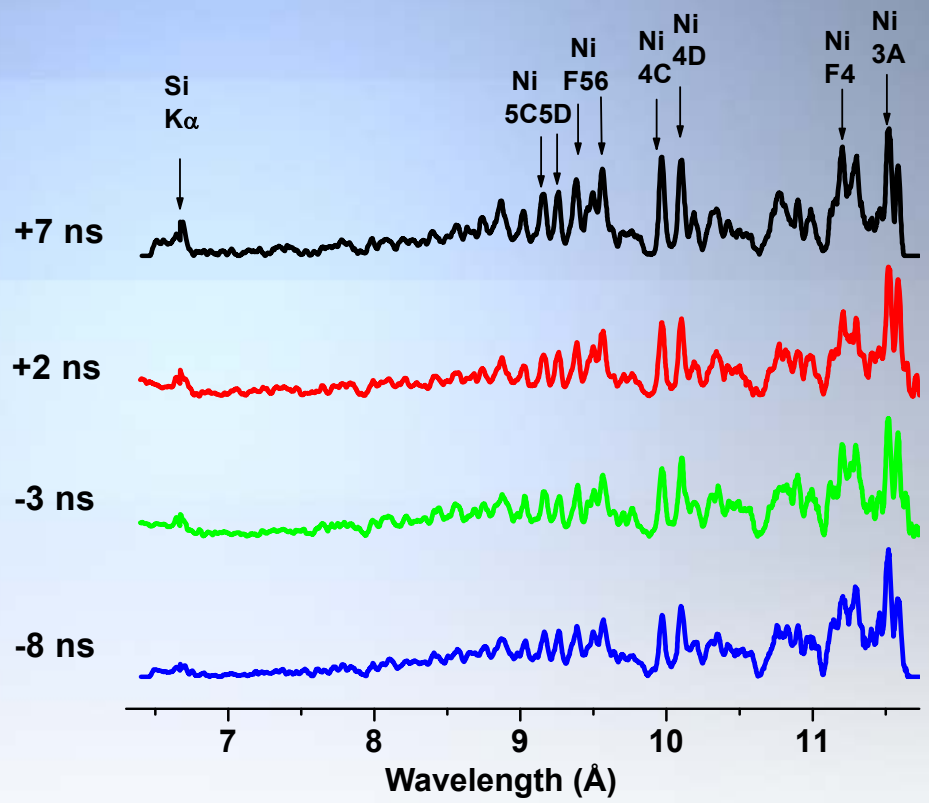

- for all recorded times, from -8 ns to 7 ns after the peak of XRD, L-shell Ni spectra look very similar
- the most intense spectral features are from Ne- , F-, and O-like ions, less intense from N-like and much less intense from C-like and Na-like ions. Te ~(350-370 eV) and Ne~(9×10^{18} cm^{-3} – 2×10^{19} cm^{-3}).

Summarizing: what ionization stages contribute to L-shell Ni before and after XRD/PCD peak in experiments at the enhanced current?

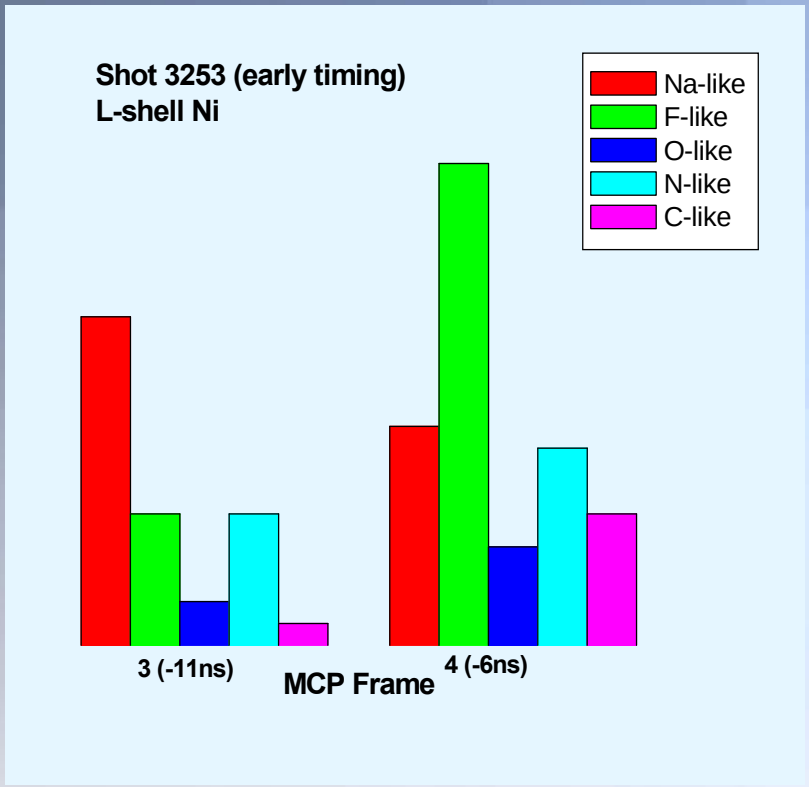

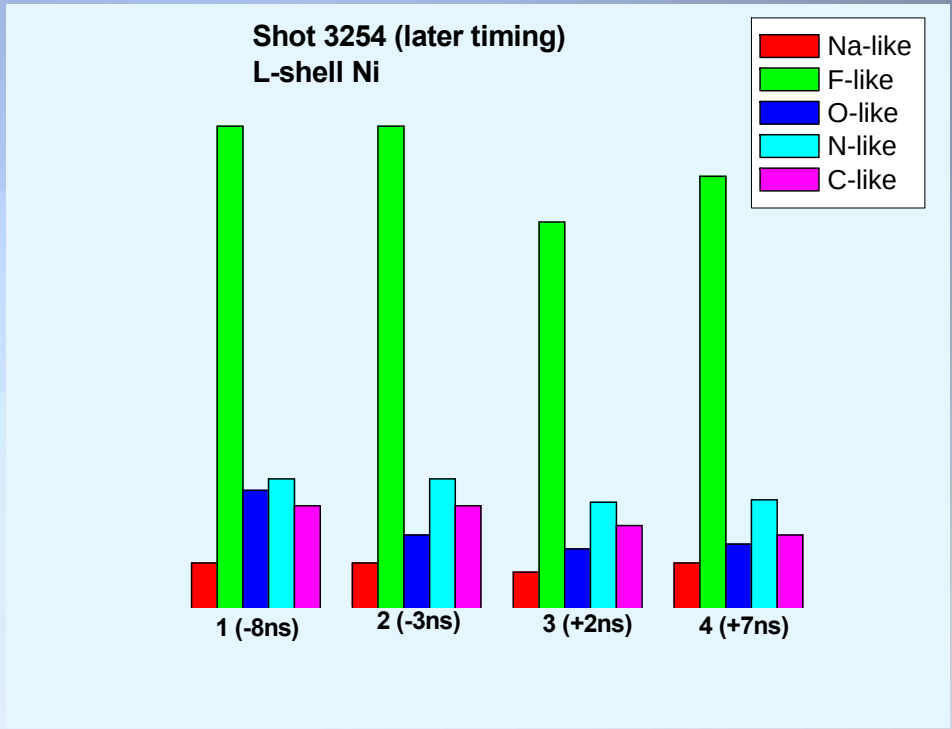

- Na-like ions dominate only early in time (frame 3 and partially frame 4 of shot 3253)
- F-like ions dominate in all frames (during the last frame of shot 3253 and from frame 1 up to 4 of shot 3254)
- The distribution of ionization states in L-shell Ni spectra does not depend on time in shot 3254

Comparison with the results at 4 MA current on Double-EAGLE[10]

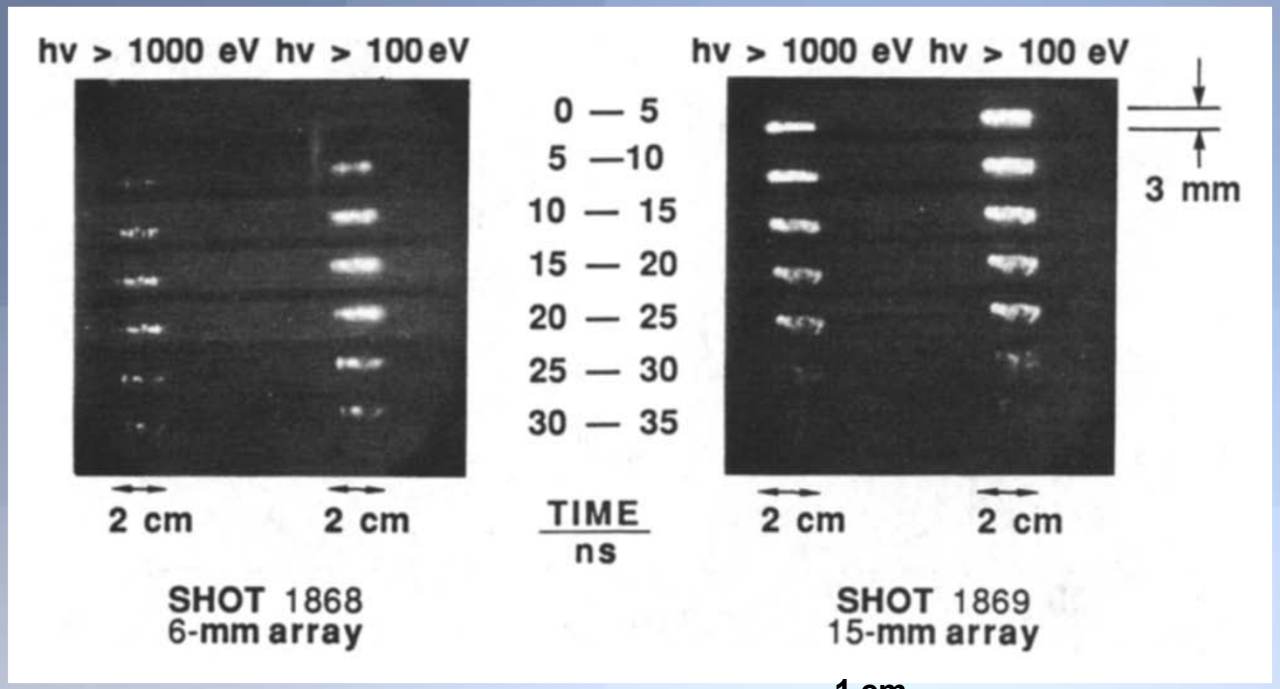

L-shell

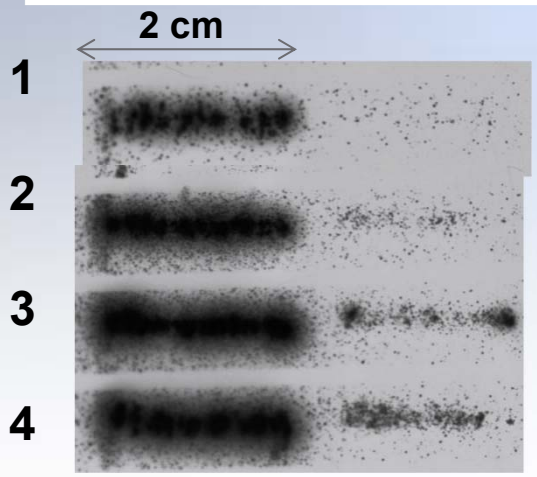

DPWA, 6 mm, 1 MA

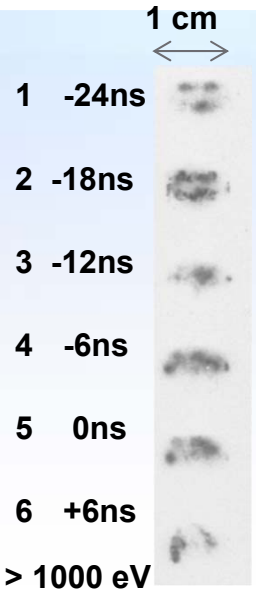

DPWA, 9 mm, 1.5 MA
- ❑ Very early radiation
- ❑ Double columns
- ❑ Hot spot-like source

[10]C. Deeney *et al*, JQSRT 44, 457 (1999)

Putting it all together for standard size DPWAs at enhanced current

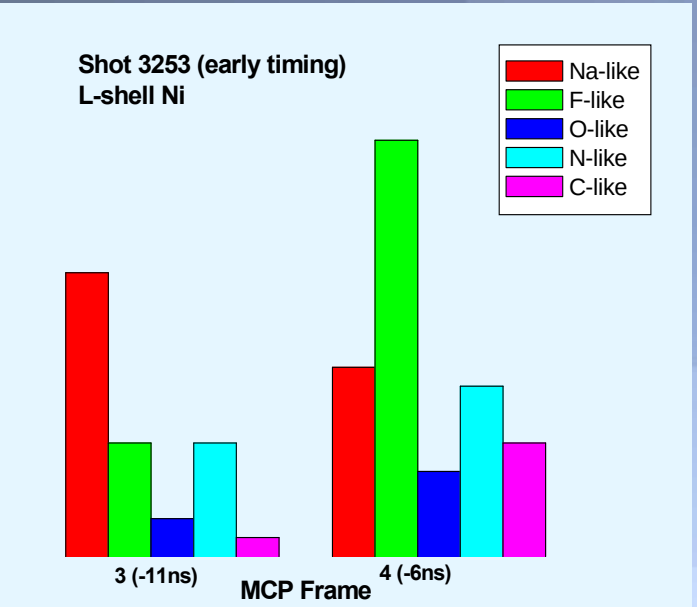

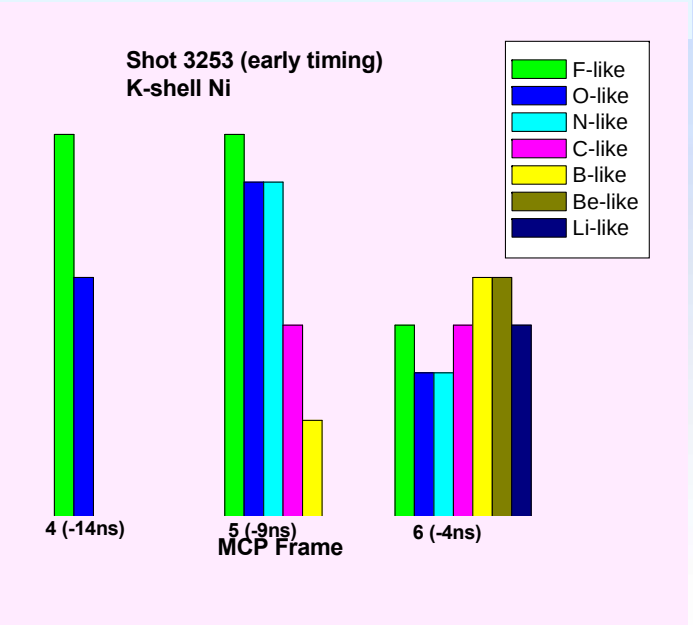

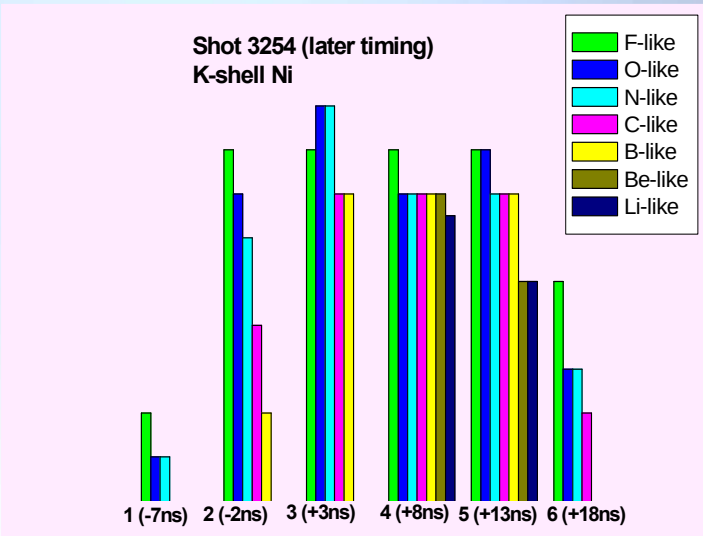

More similarities at early time

Cold Kα is generated by non-thermal electrons that spread out ionization balance over the large number of ions

Comparison with the results at 4 MA current on Double-EAGLE[9]

Double-EAGLE results (CWA)[9]

- Time-resolved diagnostics have revealed the presence of K-shell emitting hot spots within a bulk plasma with an electron temperature of a 200 eV or so.
- These results have shown that hot spots are not formed by m=0 instabilities and that they are always preceded by electron beam excited characteristic lines.
- Furthermore, increasing the electron temperature and decreasing the bulk plasma density results in the disappearance of the hot spots.

Zebra results (DPWA)

- Time-resolved diagnostics have revealed the presence of K-shell emitting regions within a bulk plasma with an electron temperature of a 320-370 eV or so.
- Time evolution of K-shell radiation of DPWAs with interplanar distance of 6 mm at 1 MA current closely resembles the Double-EAGLE results with 9 mm CWAs.
- However, time evolution of K-shell radiation of DPWAs with interplanar distance of 6 mm at the enhanced current is somewhat different. No Heα was observed but cold Kα and adjacent inner-shell lines of F- through Li-like ionization stages as well as their evolution in time.
- Unique comparison of the ionization balance of K-shell and L-shell Ni spectra of DPWAs at the enhanced current was accomplished.

[9]C. Deeney *et al*, AIP Conference Proceedings 195, 62 (1989)

SUMMARY AND ACKNOWLEDGMENTS

- We have studied implosion dynamics and radiative properties of DPWAs on the UNR's high-impedance Zebra generator (1.9Ω, 100 ns) at the enhanced current of 1.5-1.7 MA and have demonstrated:
  - the new regimes of implosions with asymmetric jets, no precursor formation, and very early radiation for larger sized arrays (Δ=9 mm, ϕ=0.54)
  - precursor formation and strong "cold" Kα emission for standard size (Δ=6 mm, ϕ=1.28) DPWAs.

- From analysis of L-shell Ni radiation, it follows that plasma conditions do not substantially change during the period of observation: F-like ions dominate shortly before and after x-ray burst.

- However, the analysis of K-shell Ni radiation demonstrates much stronger dependence on time and that the ionization balance is spread out over the large number of ions which indicates the existence of hot electrons.

- The comparison with the results produced at Double-Eagle is discussed.

This work was supported by NNSA under DOE Cooperative Agreement DE-NA0001984 and in part by DE-NA0002075.

Additional Slides

What is causing such axial asymmetries?

- It is unlikely that LCM is causing it because this effect is not observed with other loads of the same size, such as larger sized TPWAs.

- The asymmetry of implosion of DPWAs manifests through the axial asymmetry of radiation: L-shell Ni spectra are more intense in the middle between the anode and the cathode and are the weakest near the anode.

- The manifestations of axial-radiation asymmetry on SNL-Z generator were observed through the appearance of M-shell W spectra near the cathode [5]. Few mechanisms that can lead to such asymmetry were suggested including polarity effects for exploding wires in the presence of radial electric fields [5, 6].

- The radial-electric-field polarity effect was also studied in experiments at MAGPIE [7].

[5]T.W.L. Stanford *et al*, "*Evidence and mechanisms of axial-radiation asymmetry in dynamic hohlaraums driven by wire-array Z pinches*", Phys. Plasmas 12, 022701 (2005).

[6]T.W.L. Stanford *et al* "*Wire initiation critical for radiation asymmetry in Z-pinch-driven dynamic hohlaraums*", Physical Review Letters 98, 065003 (2007).

[7] S.N. Bland *et al*, "*Effect of Radial-Electric-Field Polarity on Wire-Array Z-Pinch Dynamics*", *Physical Review Letters 95, 135001 (2005).*